

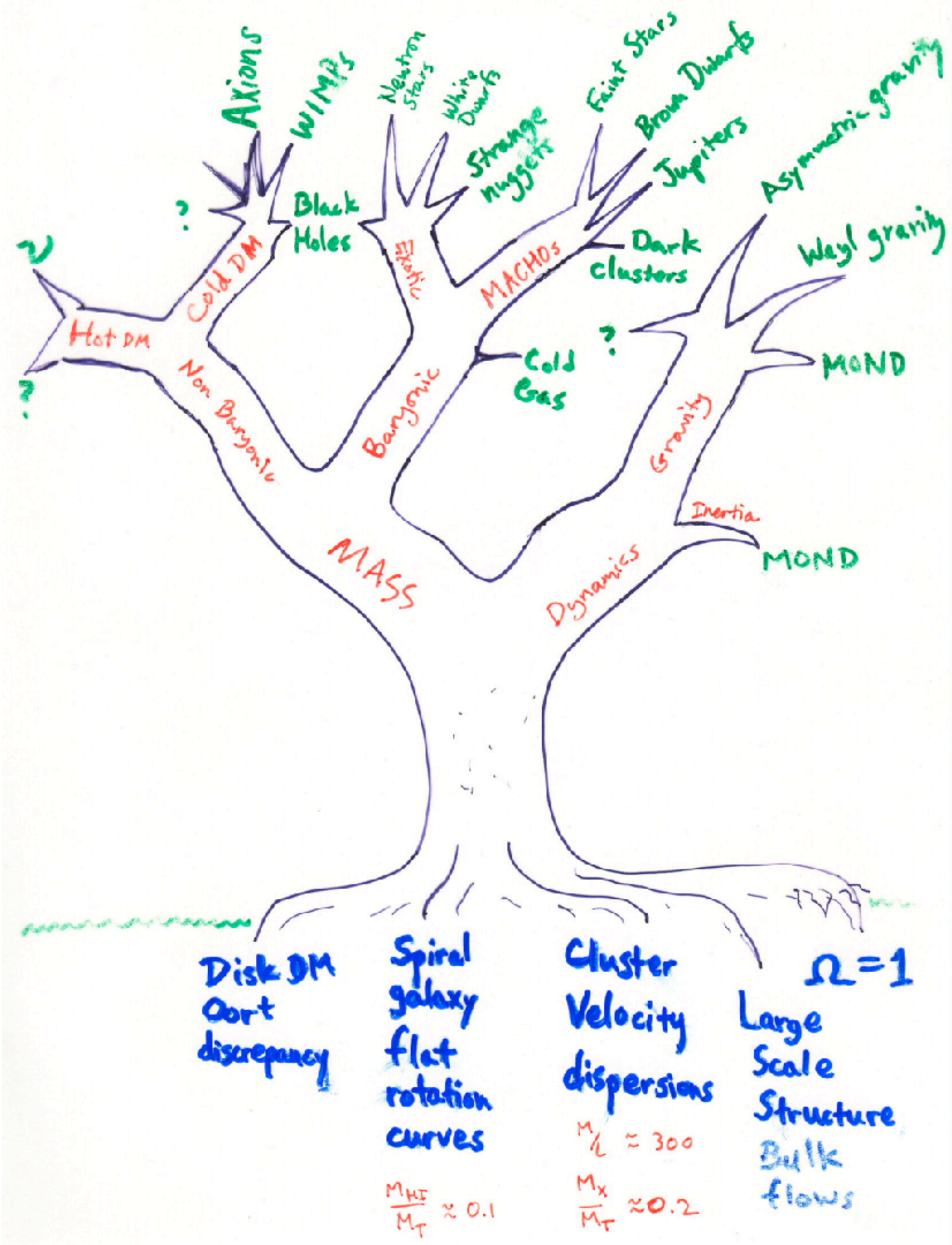
DARK MATTER

ASTR 333/433
 SPRING 2026
 TR 11:30AM-12:45PM
 SEARS 552

<http://astroweb.case.edu/ssm/ASTR333/>

PROF. STACY MCGAUGH
 SEARS 558
 368-1808

stacy.mcgaugh@case.edu



A JWST First Release image of Cluster SMACS 0723. The image shows a dense field of galaxies, many of which are distorted and stretched into arcs and multiple images due to gravitational lensing. The galaxies are primarily orange and red, with some blue stars scattered throughout. A prominent bright star in the upper center has a complex pattern of diffraction spikes. The background is dark, highlighting the individual galaxies and their distorted shapes.

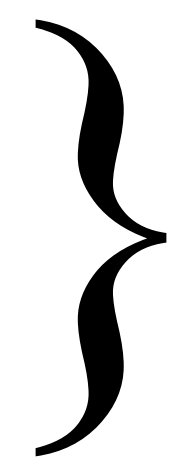
JWST First Release image
Gravitational lensing in
Cluster SMACS 0723

Four distinct measures:
velocity dispersion, hydrostatic equilibrium of X-ray gas, the Sunyaev-Zel'dovich effect, and gravitational lensing

Gravitational Lensing

Flavors of gravitational lensing:

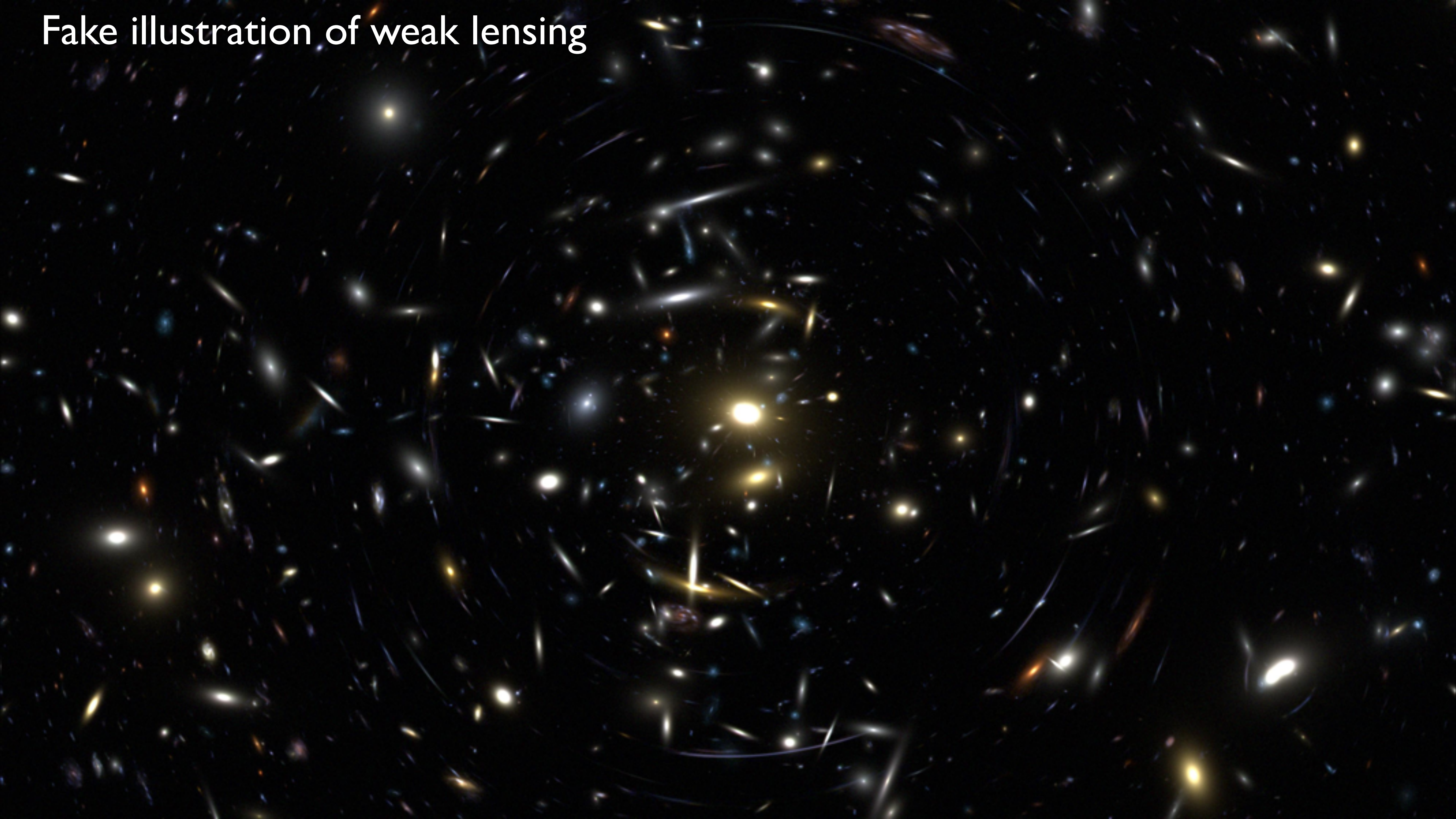
- weak lensing
mild distortion of lensed image
- strong lensing
multiple images, strong distortion
- microlensing
temporary brightening due to unresolved lensing



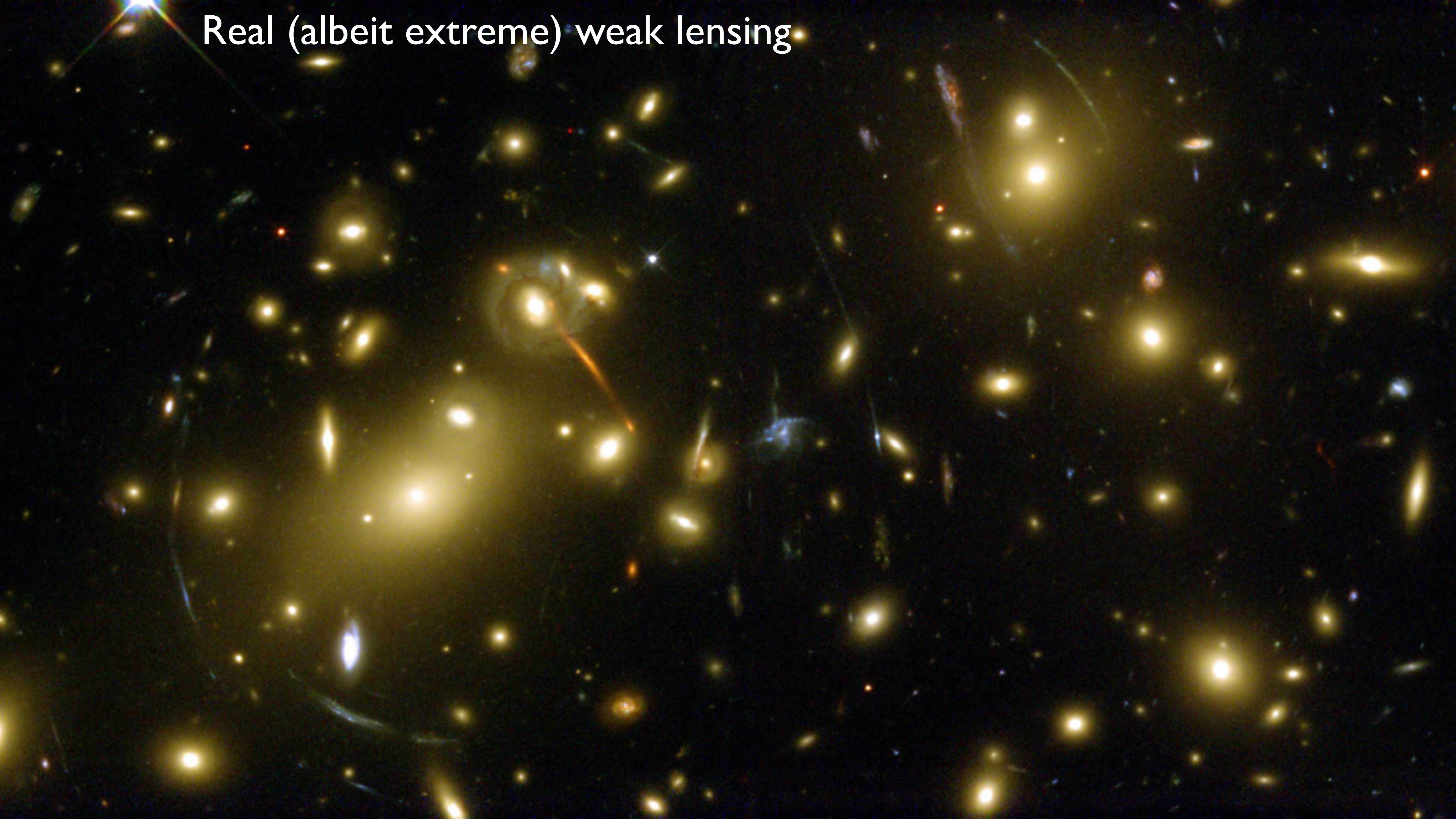
separated by the critical surface density

$$\Sigma_{\text{crit}} = \frac{c^2}{4\pi G} \frac{D_S}{D_L D_{LS}}$$

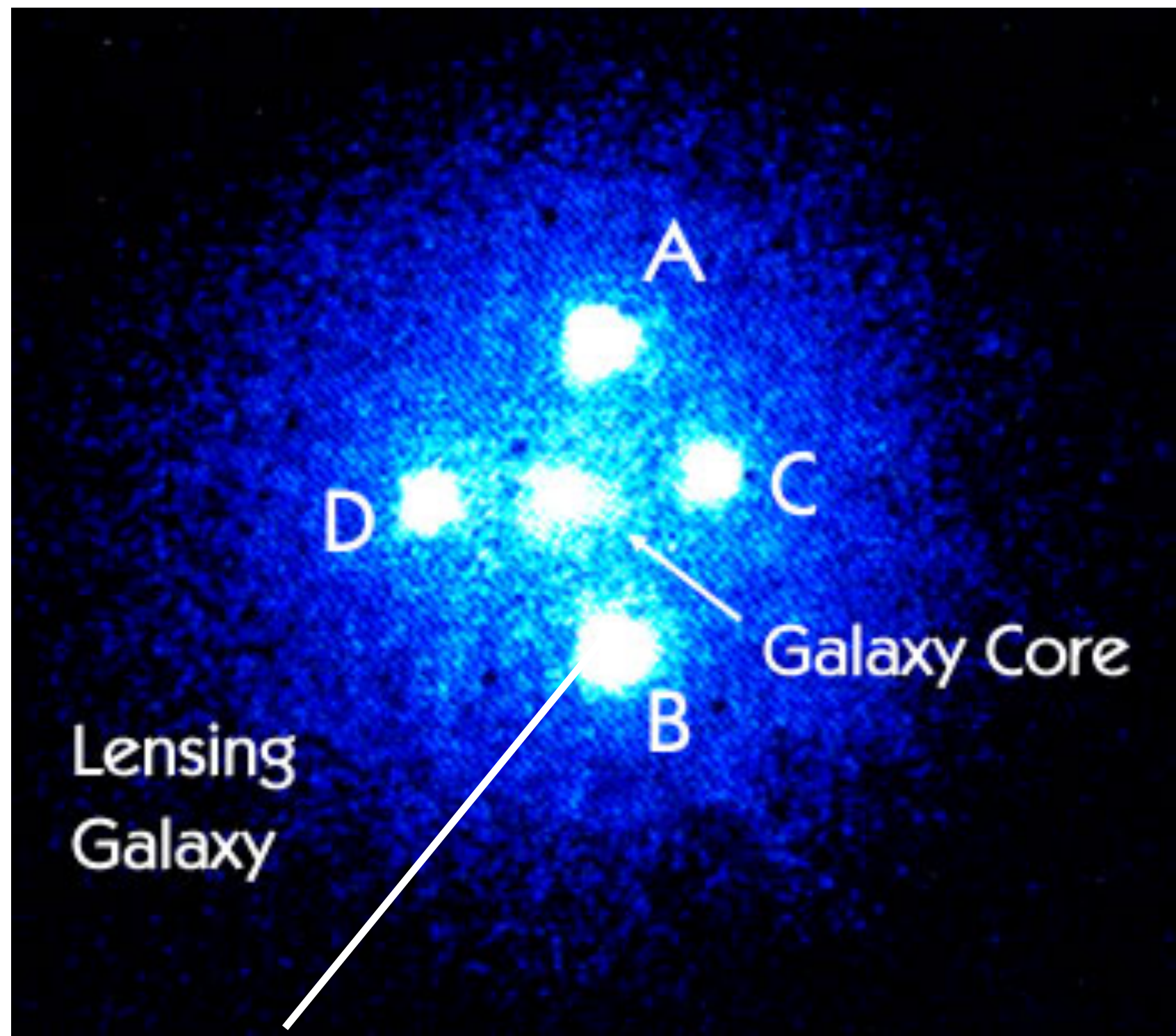
Fake illustration of weak lensing



Real (albeit extreme) weak lensing

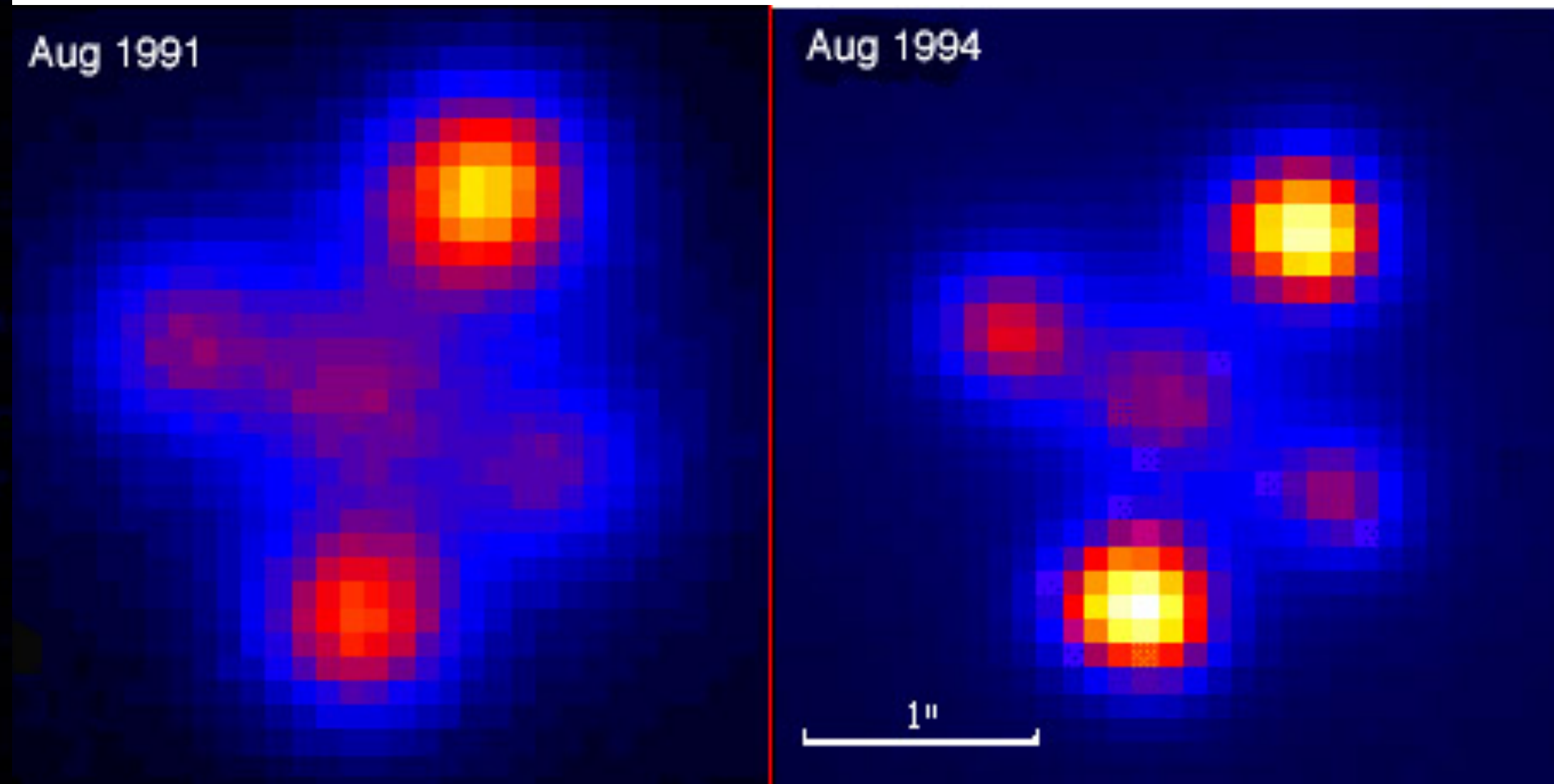


The Einstein Cross



ABCD: same QSO seen 4 times

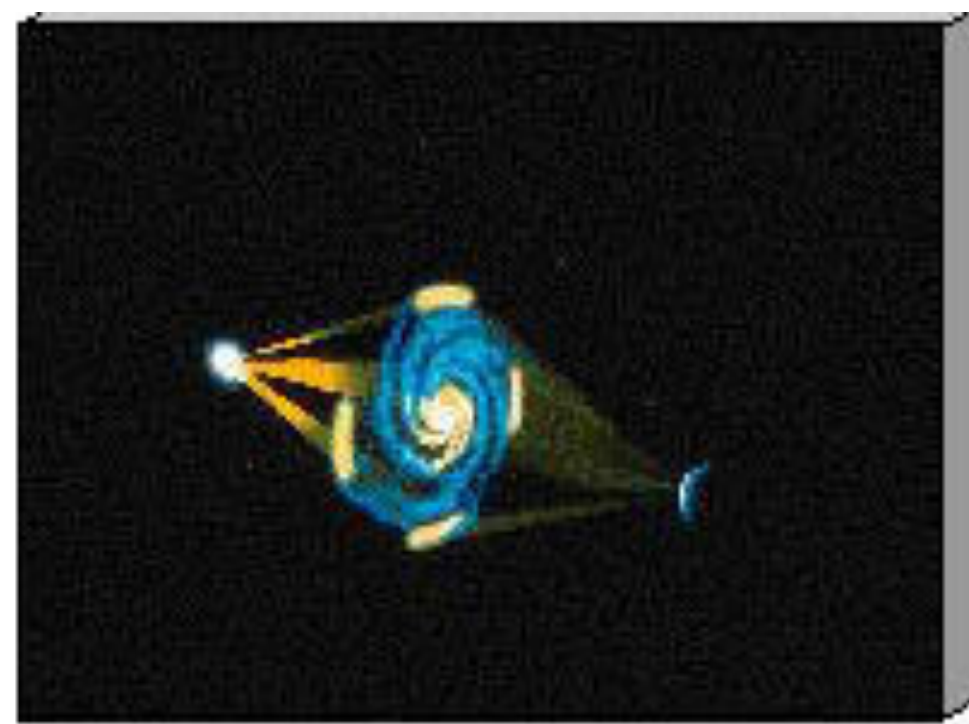
Multiple images from **strong lensing**



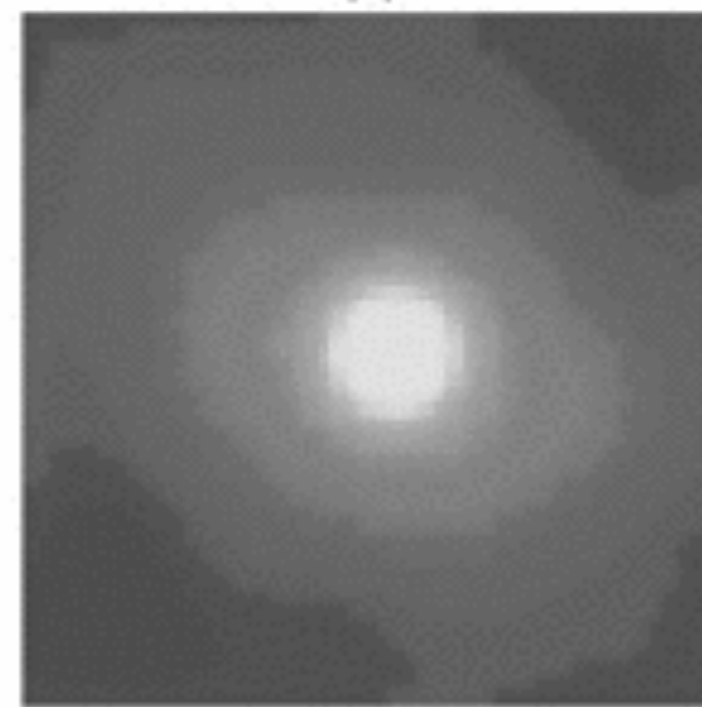
time variable multiple QSO image



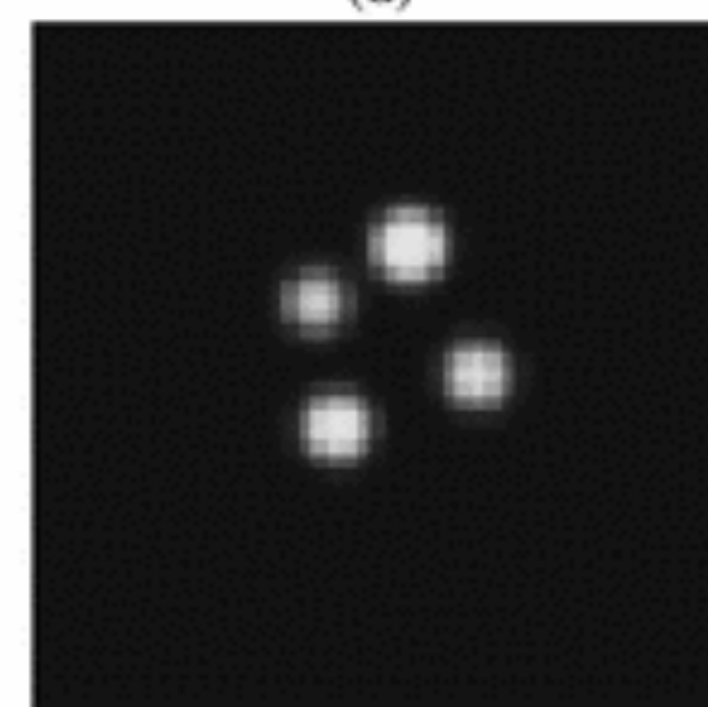
(a)



(b)



lensing galaxy



lensed QSO

Gravitational Lensing

θ_I observed angle between image and lens

D_L lens distance

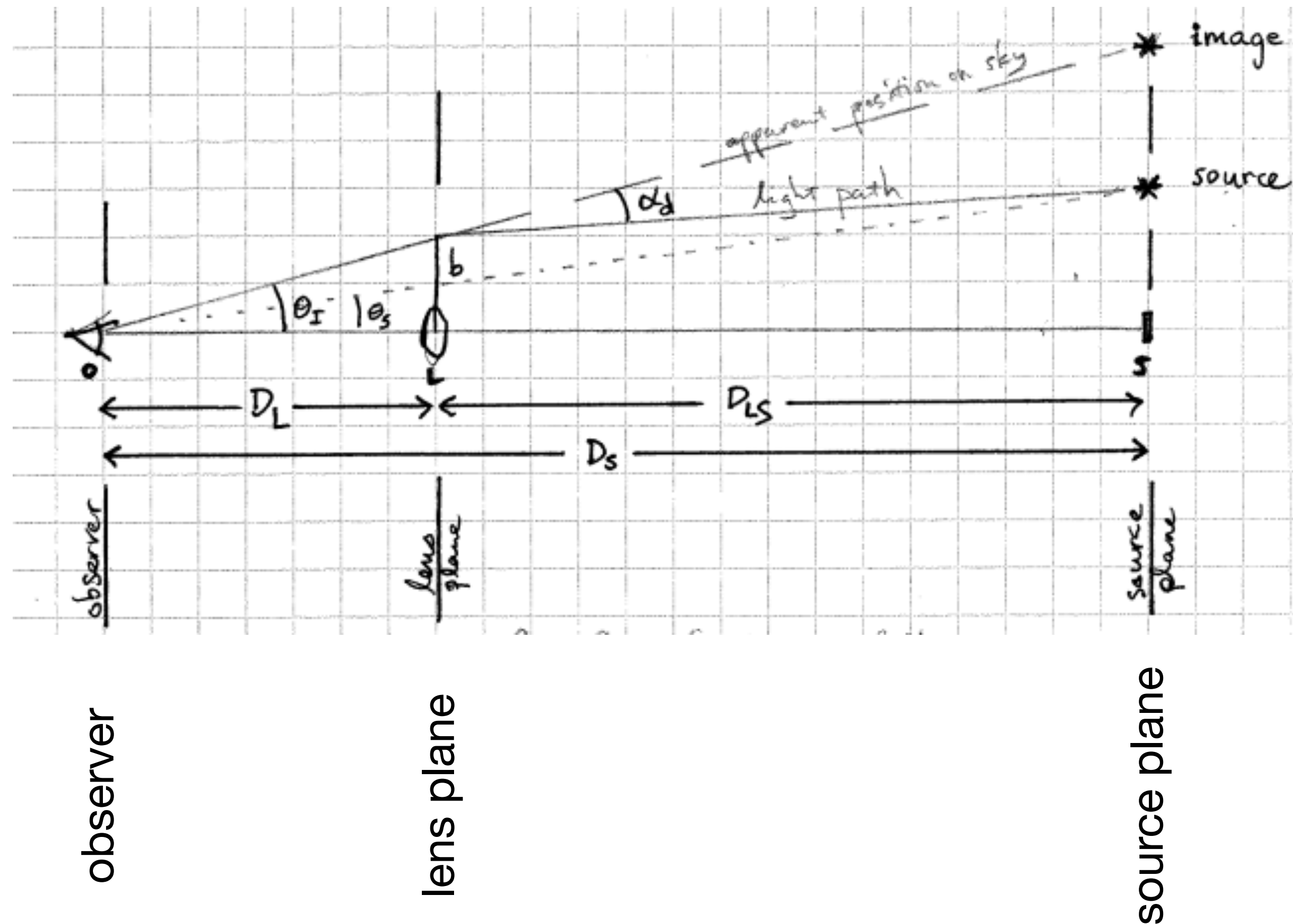
θ_S true separation angle between image and lens

D_S source distance

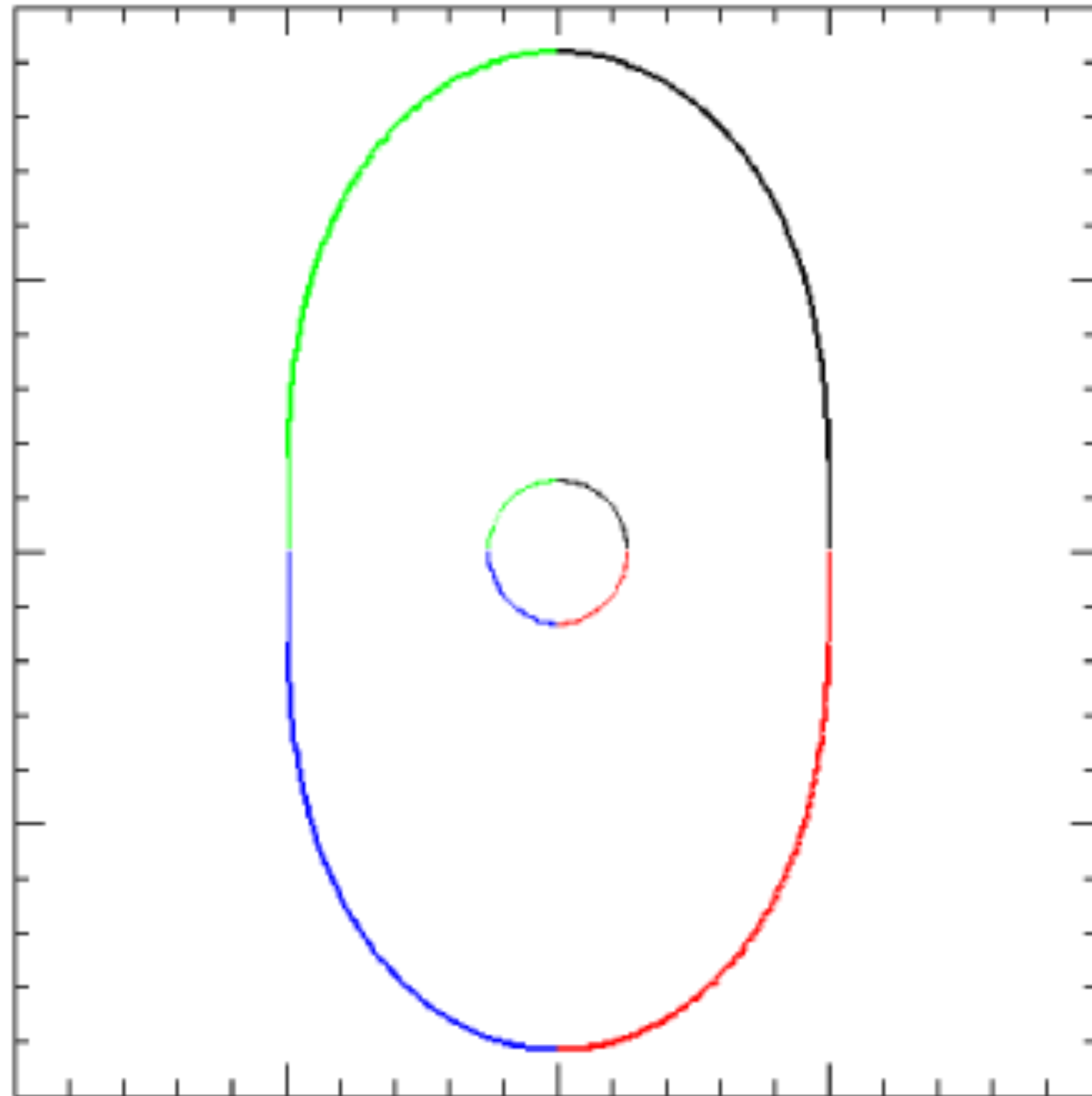
α_d bend angle

D_{LS} lens-source separation

b impact parameter



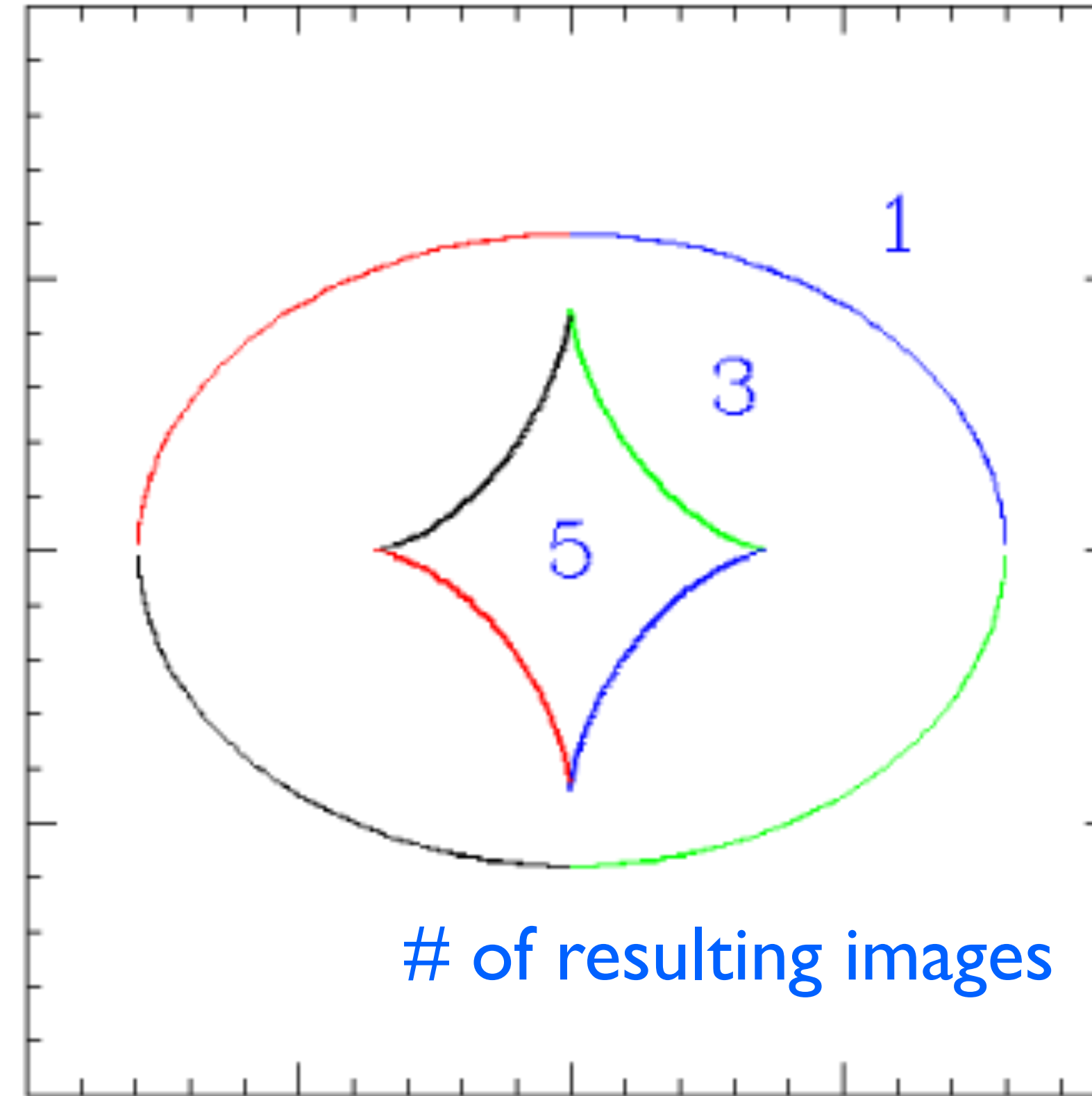
Lens plane



critical curves

Critical curves are the lines in the lens plane where the magnification diverges towards infinity.

Source plane

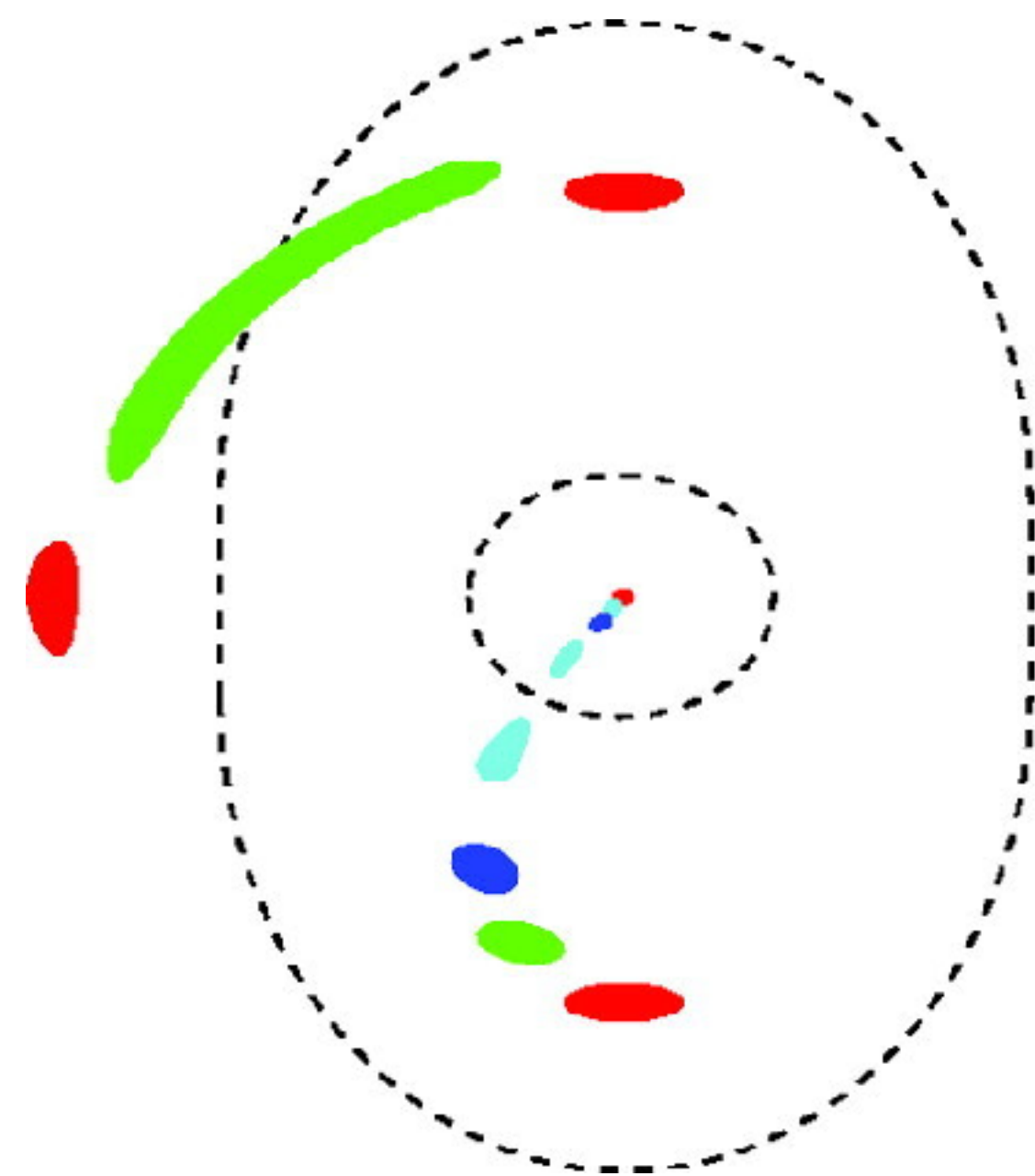


of resulting images

caustics

Caustics are the corresponding lines in the source plane where the critical surface density Σ_{crit} is reached. Traced back from the observer, multiple light rays bunch up, causing high magnification.

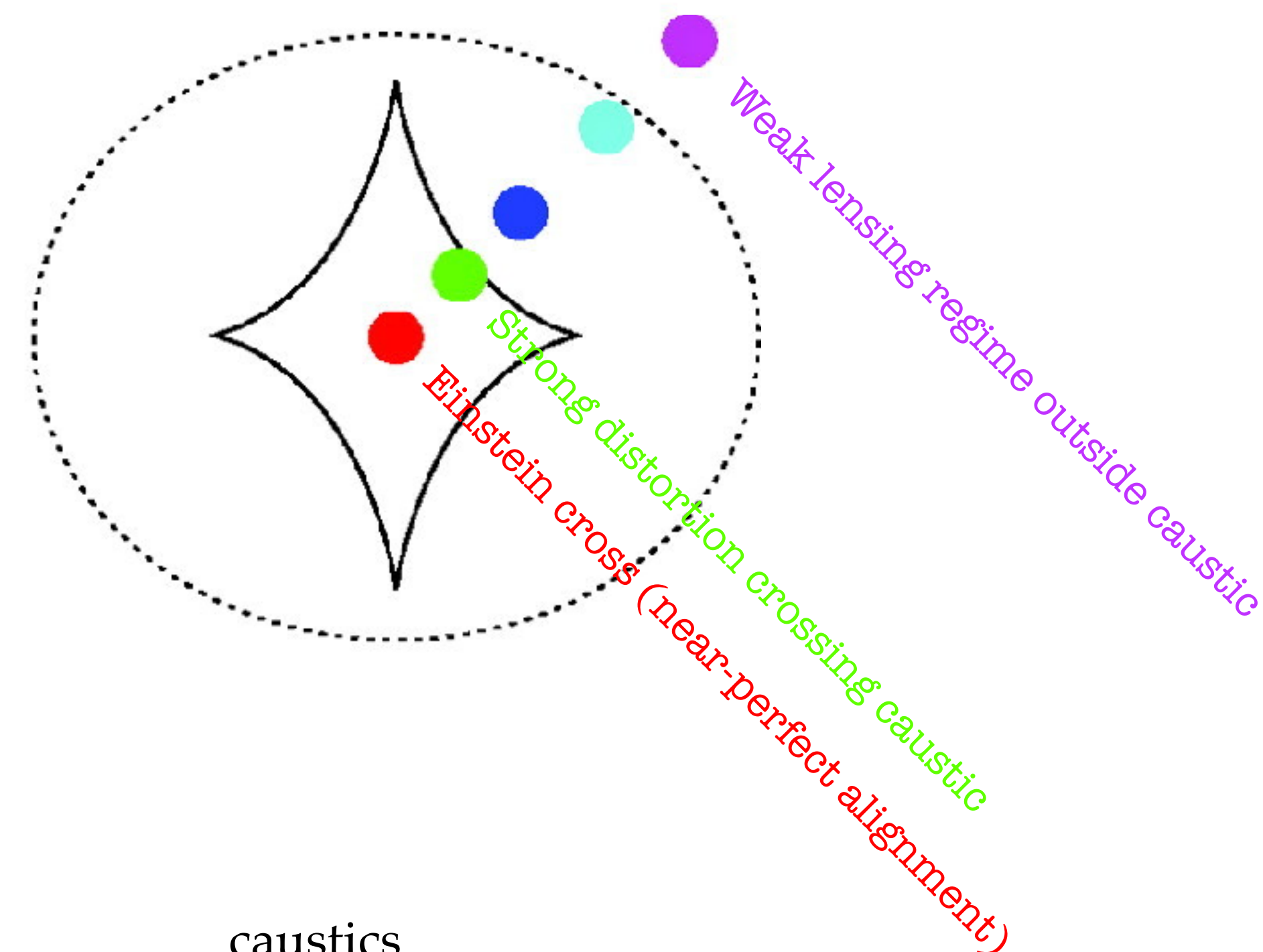
Lens plane



critical curves

Critical curves are the lines in the lens plane where the magnification diverges towards infinity.

Source plane

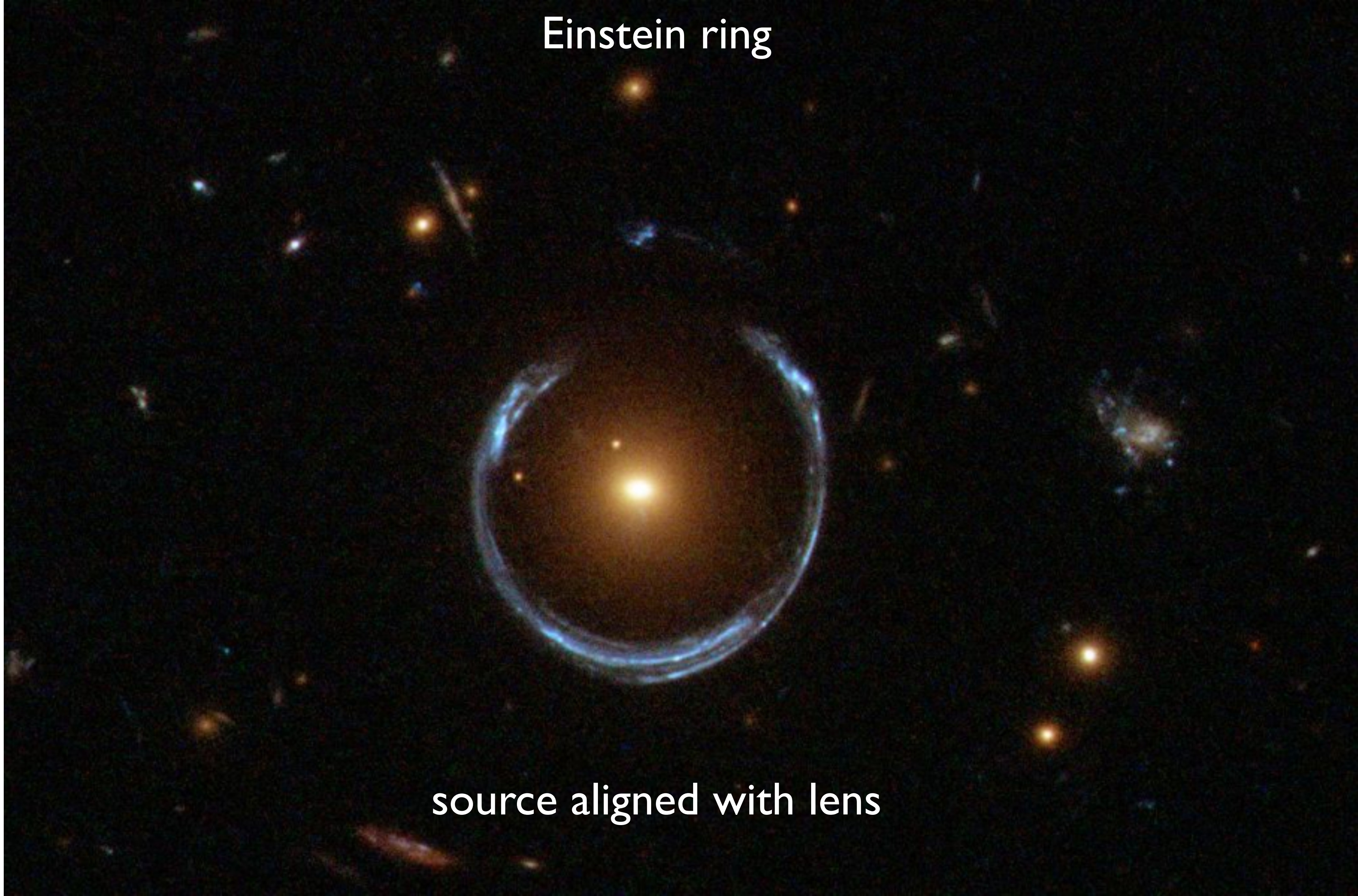


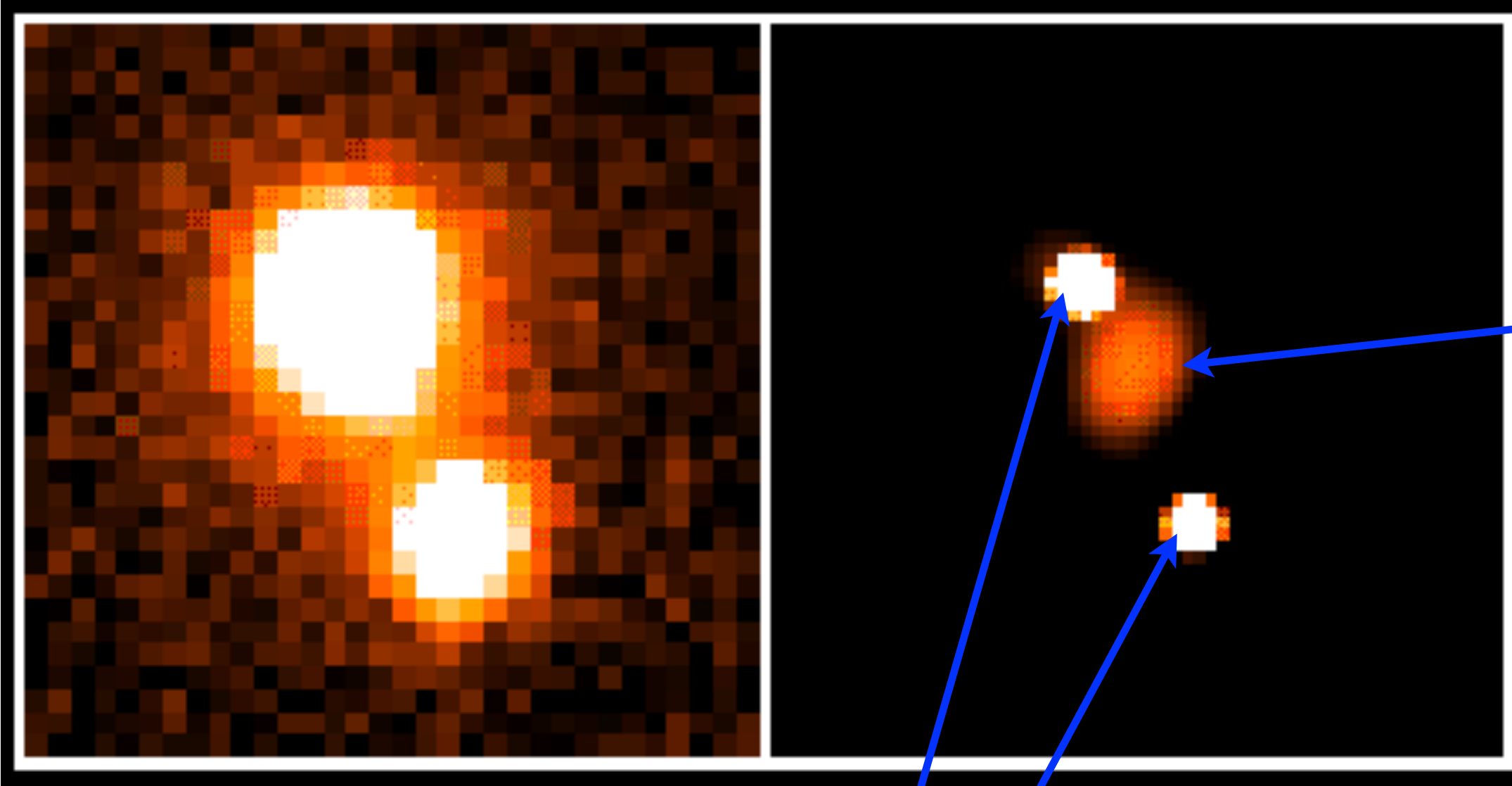
caustics

Caustics are the corresponding lines in the source plane. Traced back from the observer, multiple light rays bunch up, causing high magnification.

Einstein ring

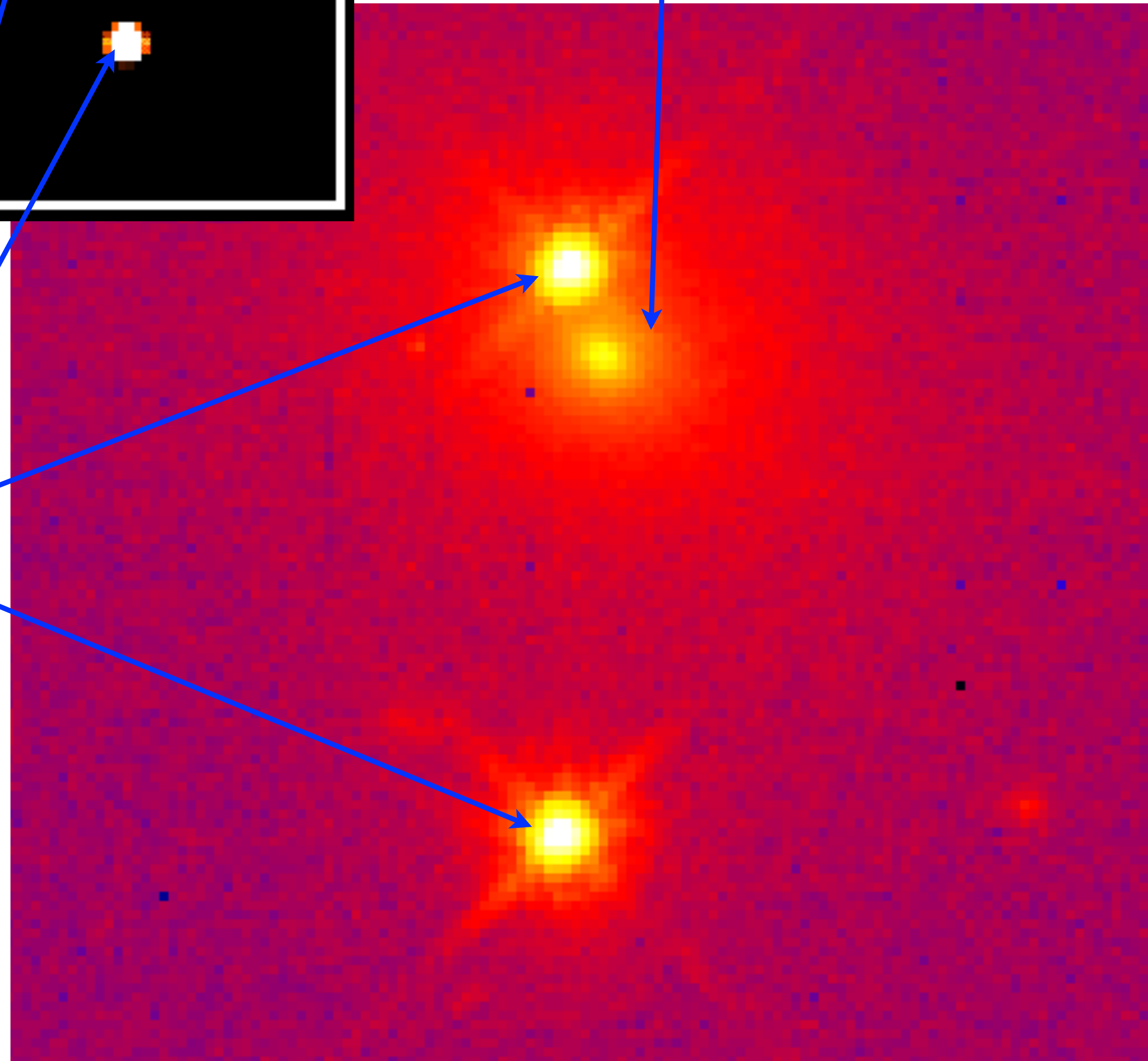
source aligned with lens



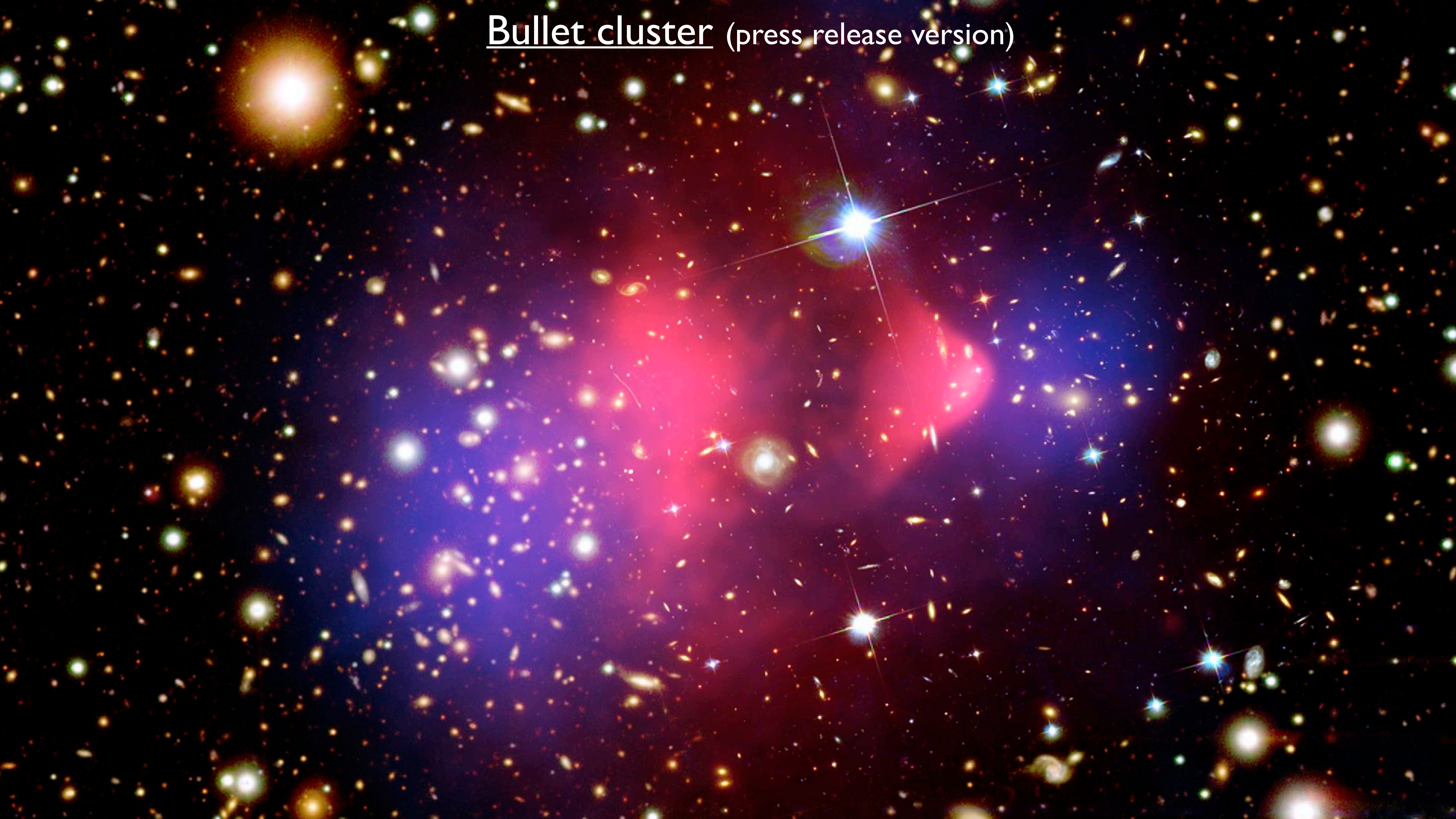


Lensing galaxy

Lensed images

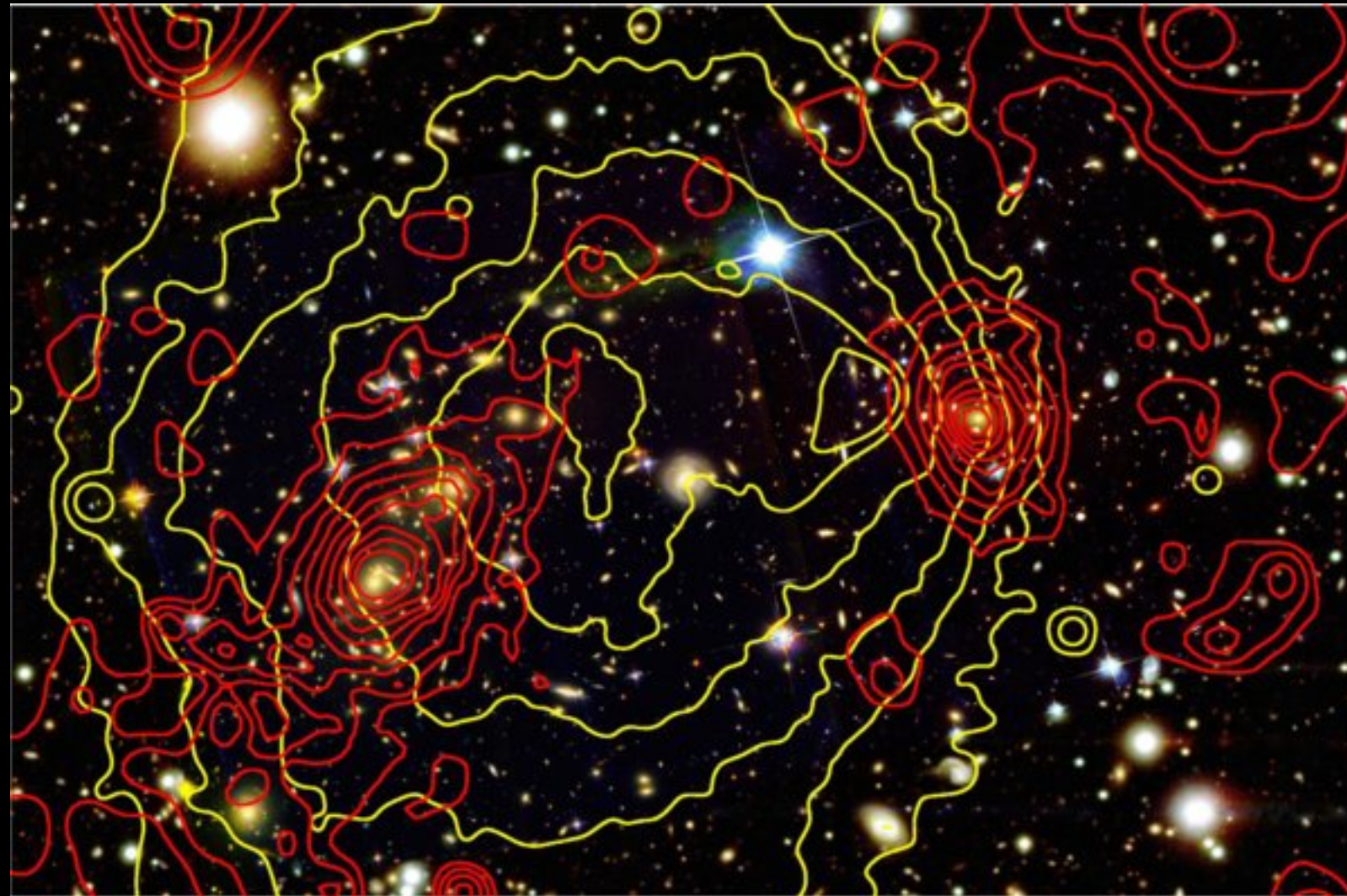


Bullet cluster (press release version)



Bullet cluster (data: Bradac et al. 2009)

X-ray: yellow contours



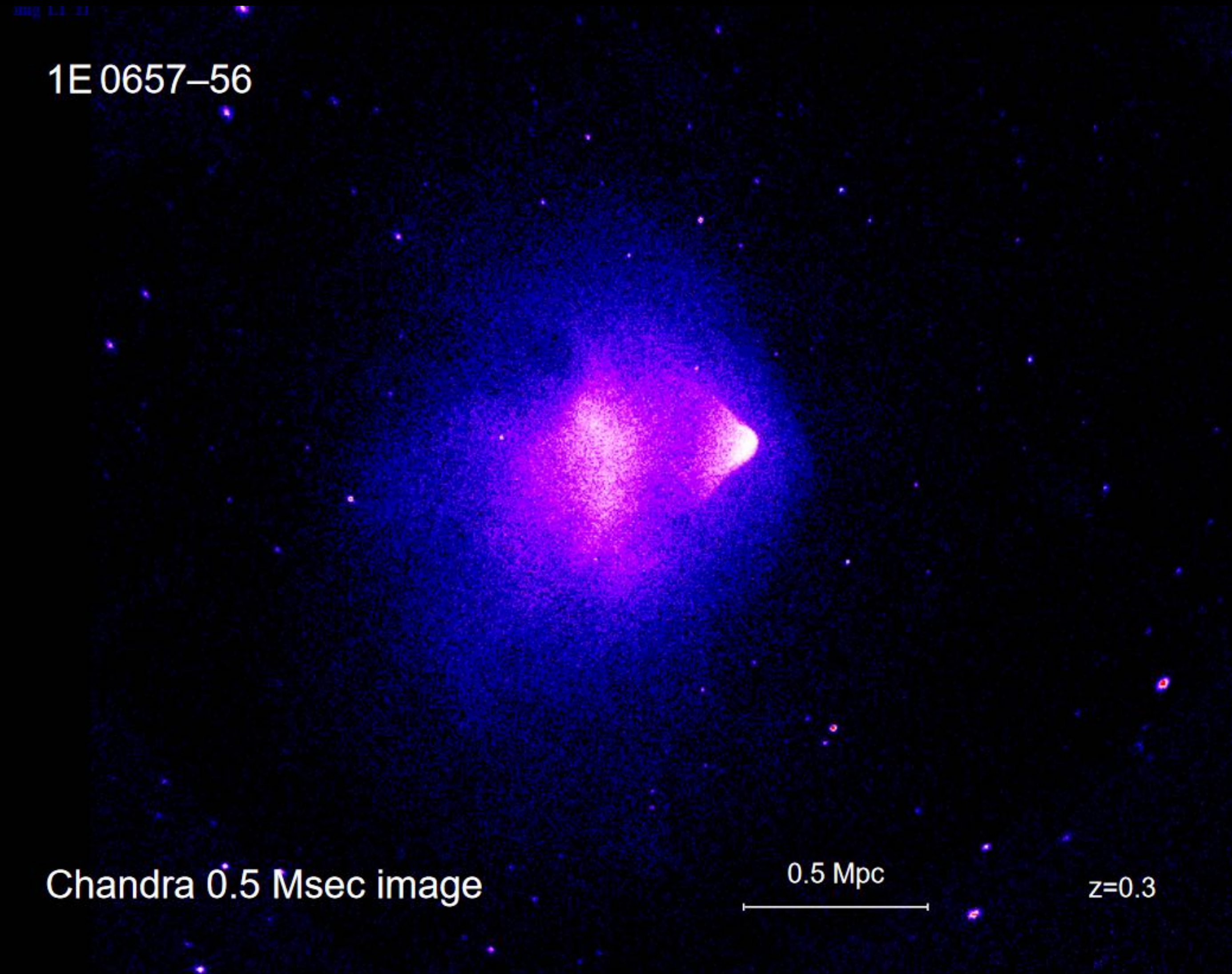
gravitational (strong+weak)
lensing: red contours

1E 0657-56

Chandra 0.5 Msec image

0.5 Mpc

$z=0.3$

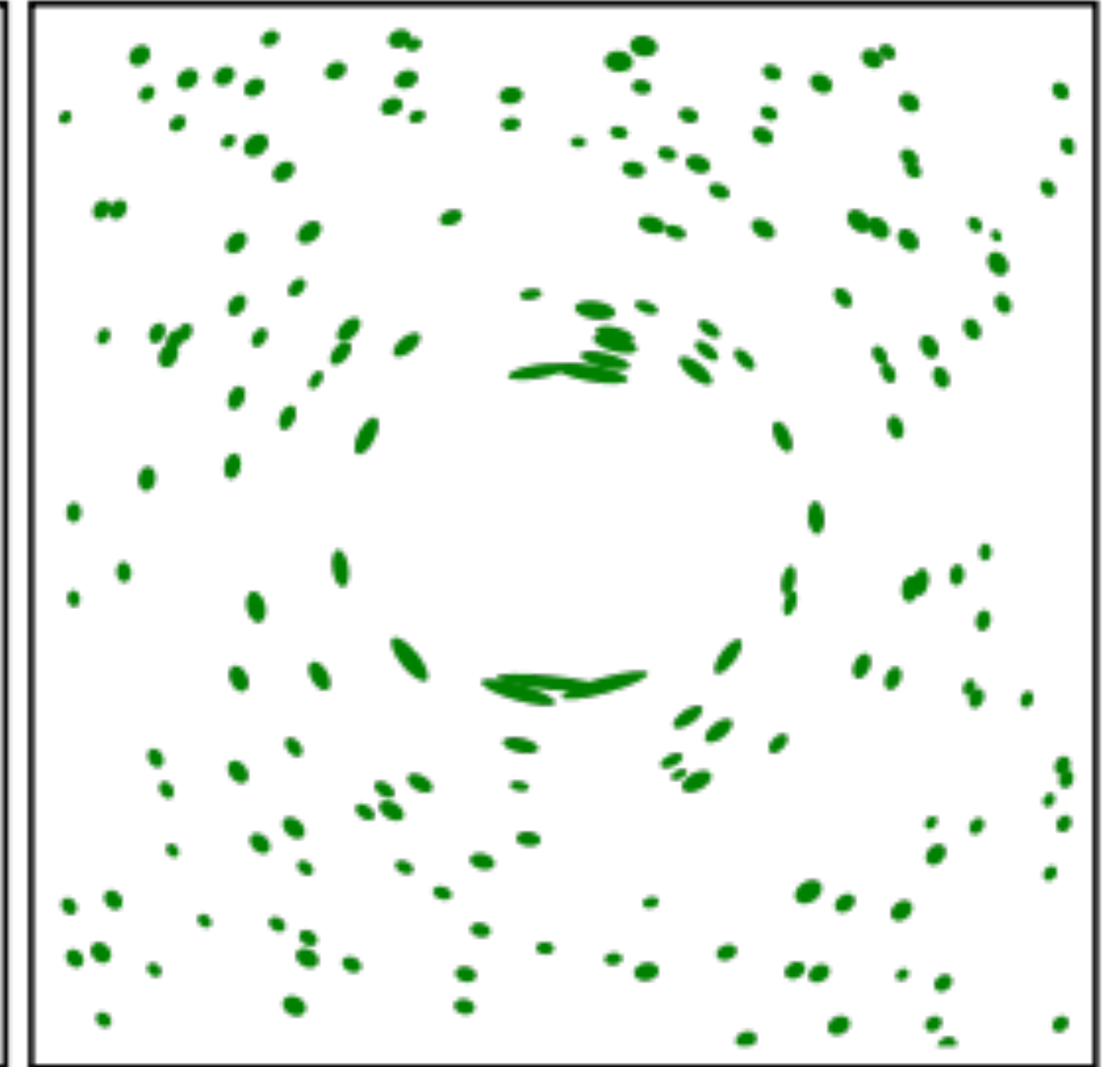
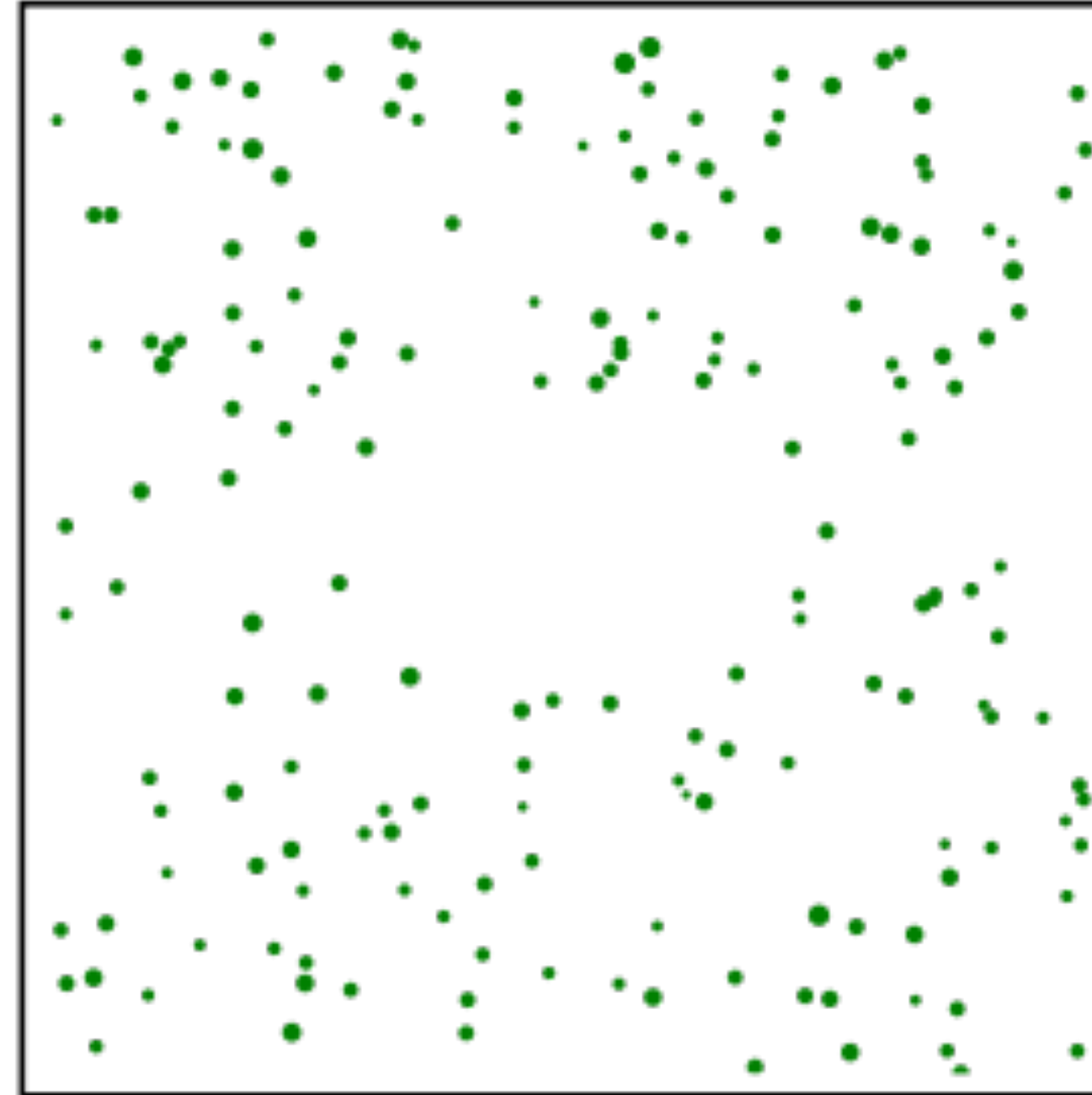


weak gravitational lensing

Unlensed

Lensed

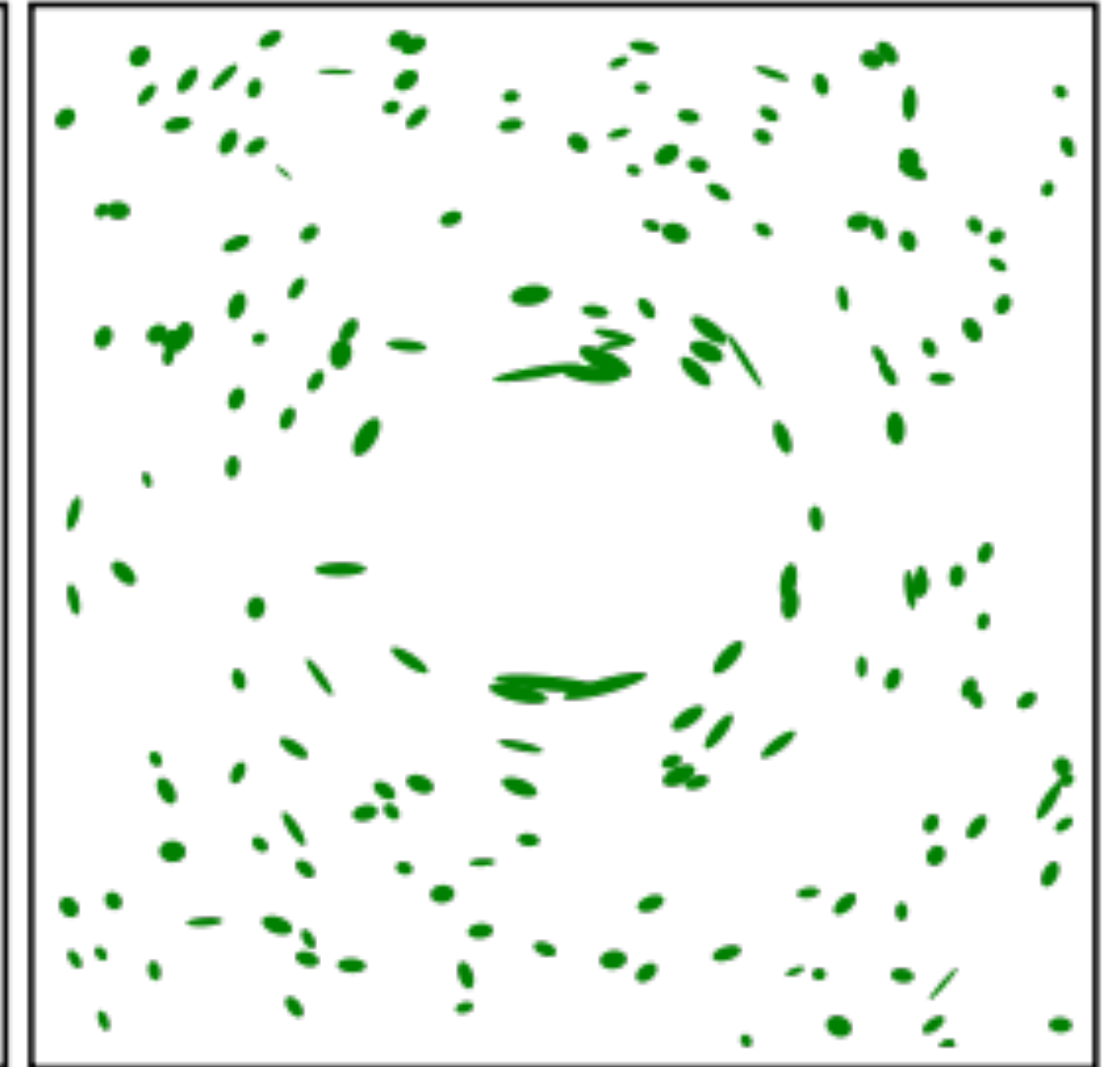
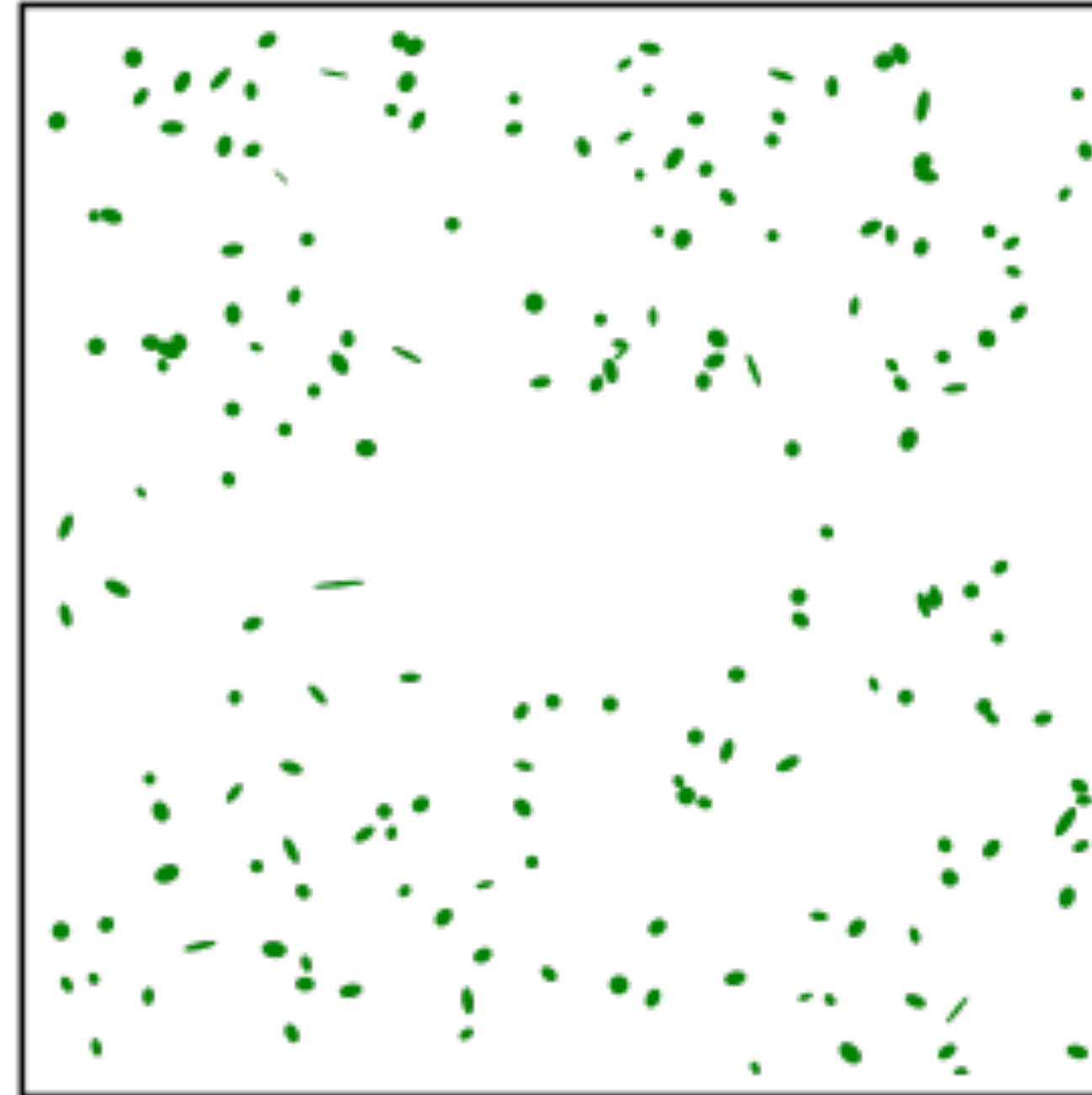
Without Shape Noise



statistical estimation from large surveys

constrain the shear across the sky
which is related to the excess
surface density of lensing

With Shape Noise



Gravitational Lensing

θ_I observed angle between image and lens

D_L lens distance

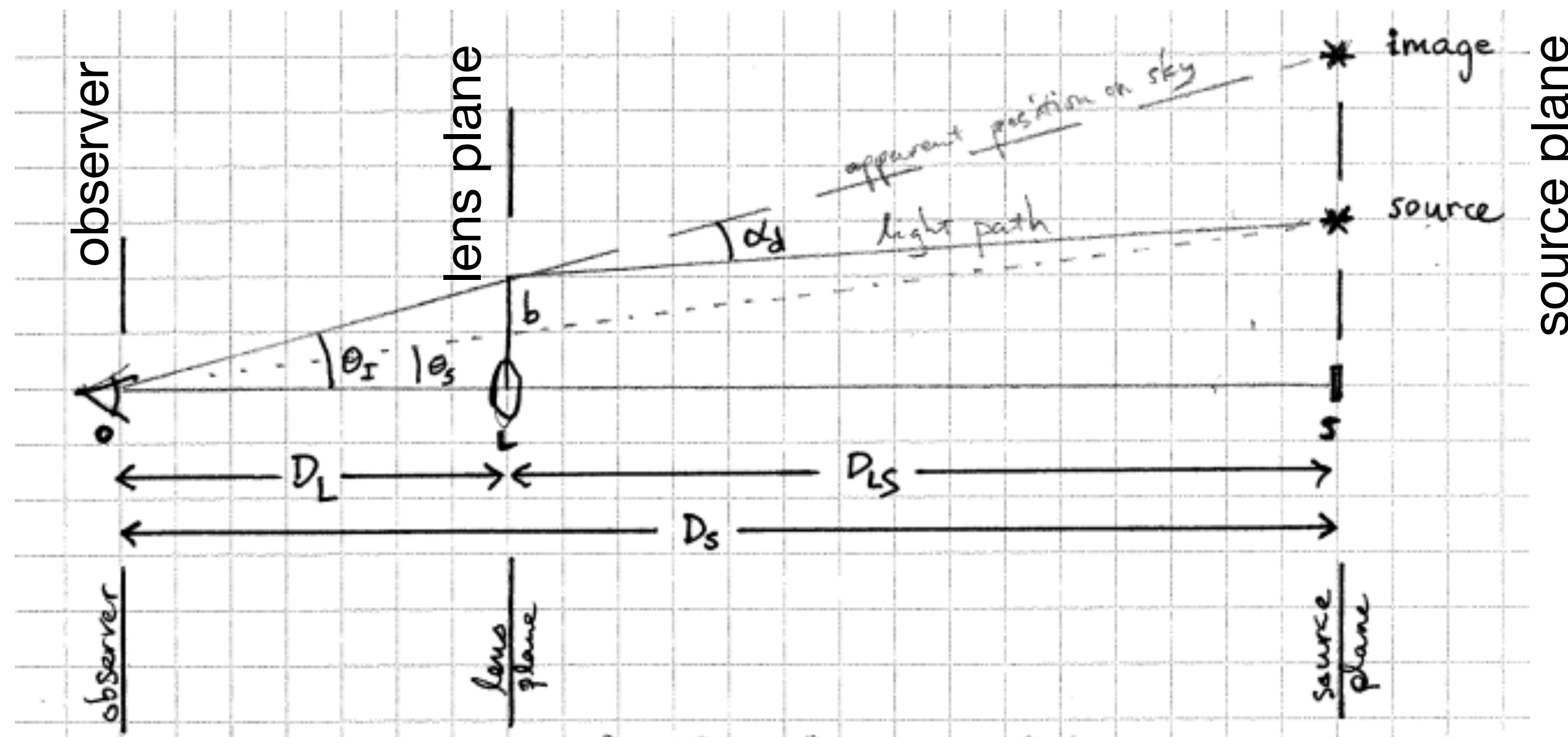
θ_S true separation angle between image and lens

D_S source distance

α_d bend angle

D_{LS} lens-source separation

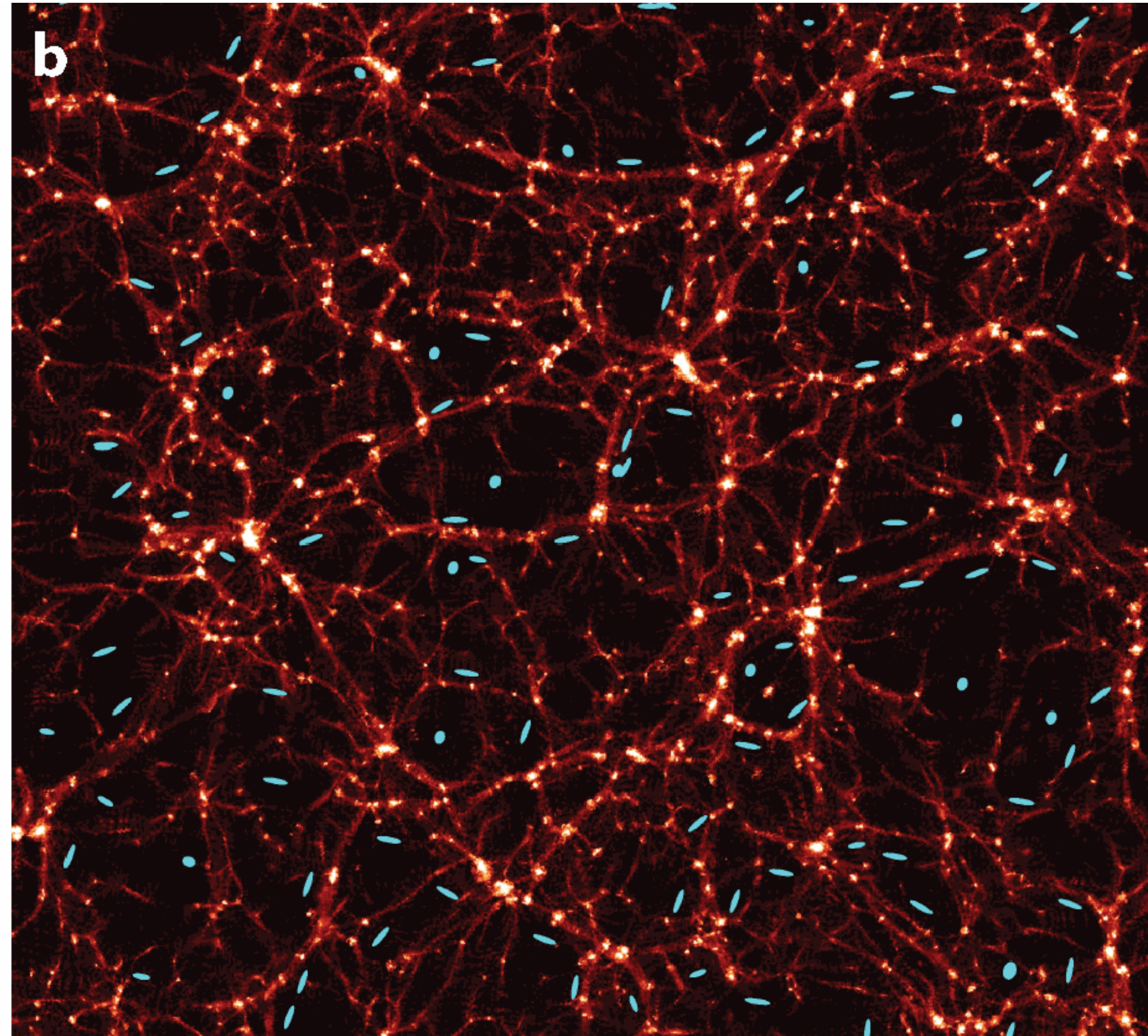
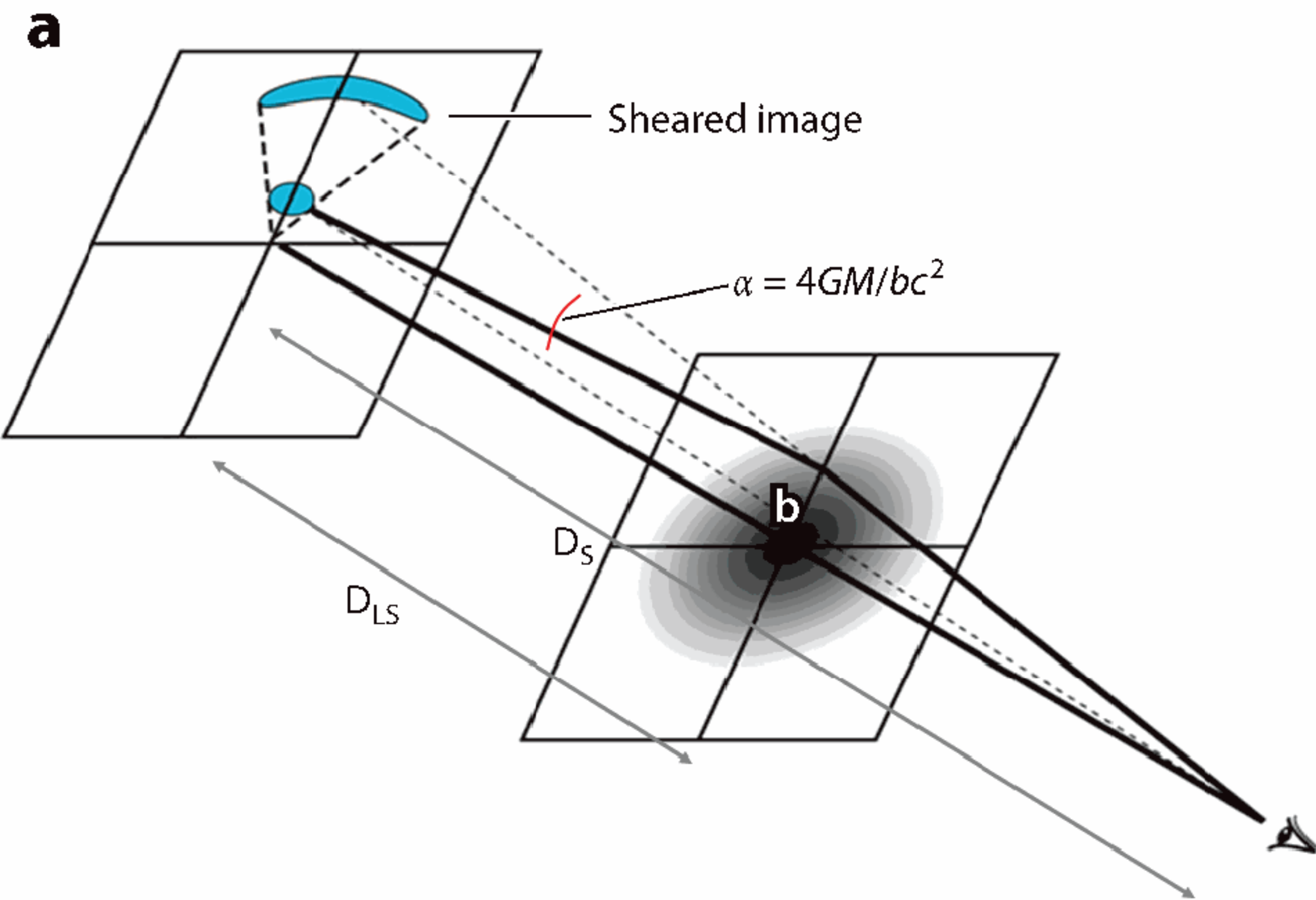
b impact parameter



weak lensing

mass enclosed by angle Θ_I : $M(< \Theta_I) = (1.1 \times 10^{14} M_{\odot}) \left(\frac{\Theta_I}{30''} \right)^2 \left(\frac{D_L}{D_S} \right) \left(\frac{D_{LS}}{1 \text{ Gpc}} \right)$ scaled for clusters of galaxies

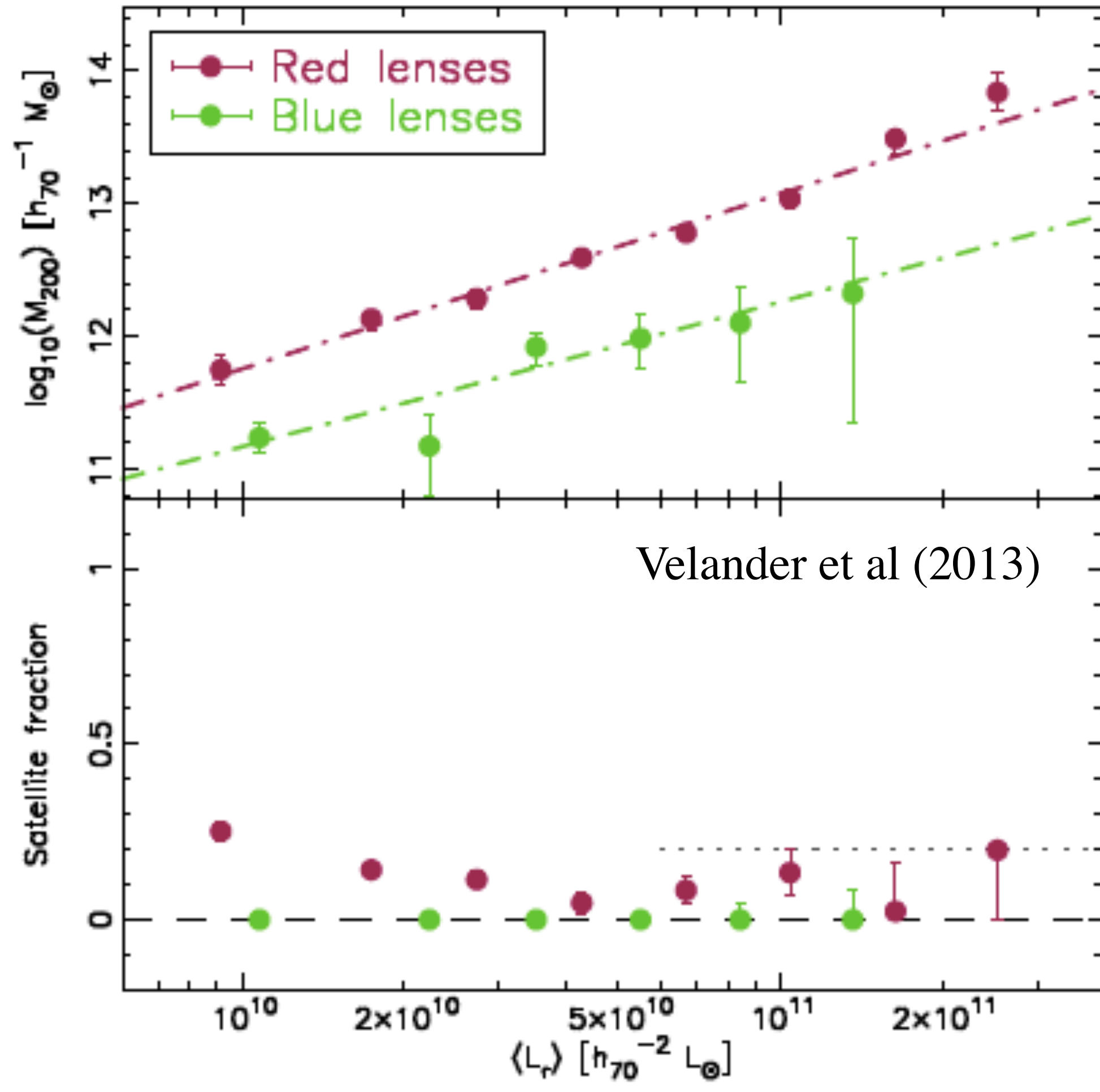
weak gravitational lensing



statistical estimation from large surveys

e.g., EUCLID

BIG SCALES
average shear across the universe



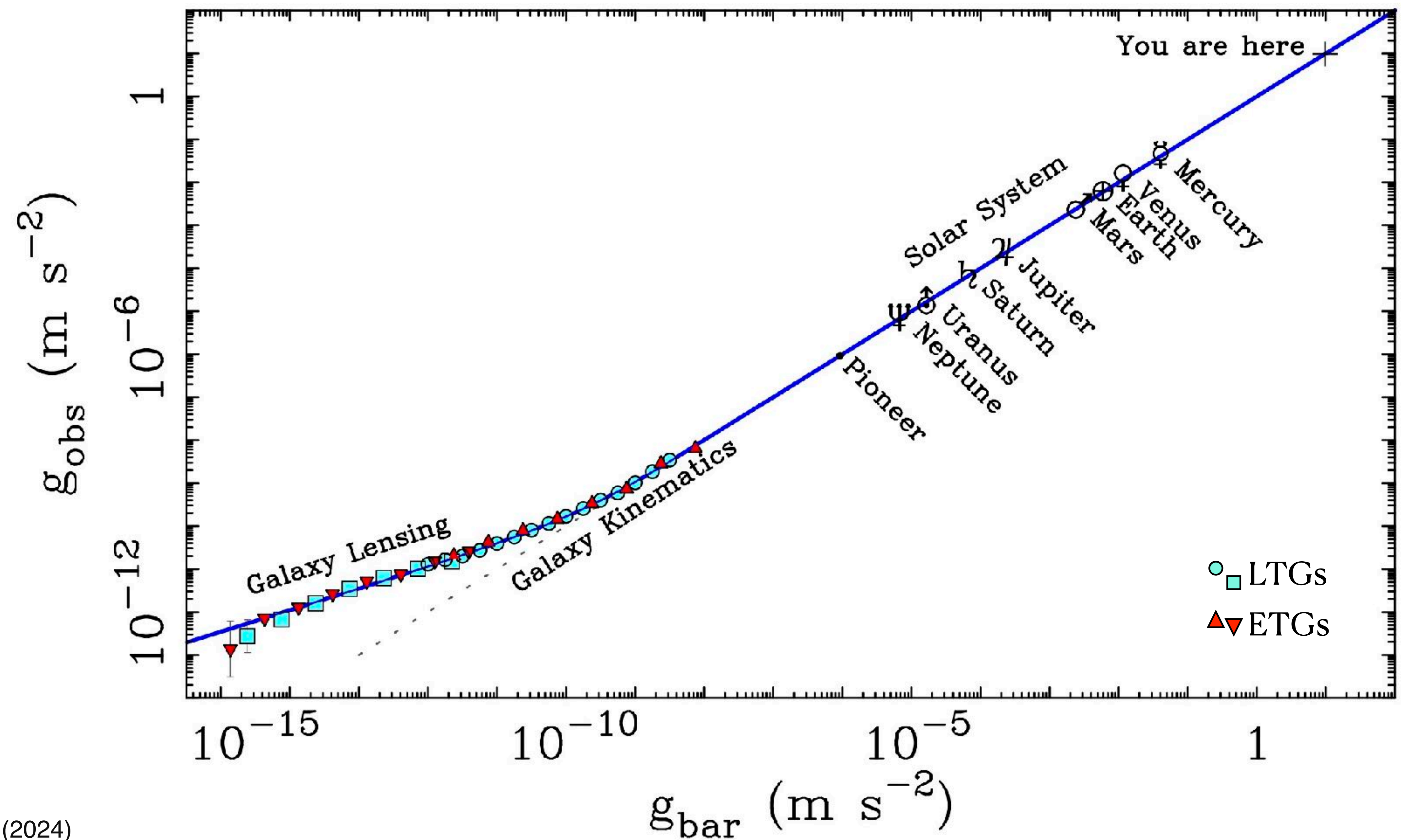
Weak lensing provides a statistical constraint on the total halo mass

see also
 Brimiouille et al (2013)

$$M_{200} = 119 L_r^{1.32} \quad \text{for red galaxies}$$

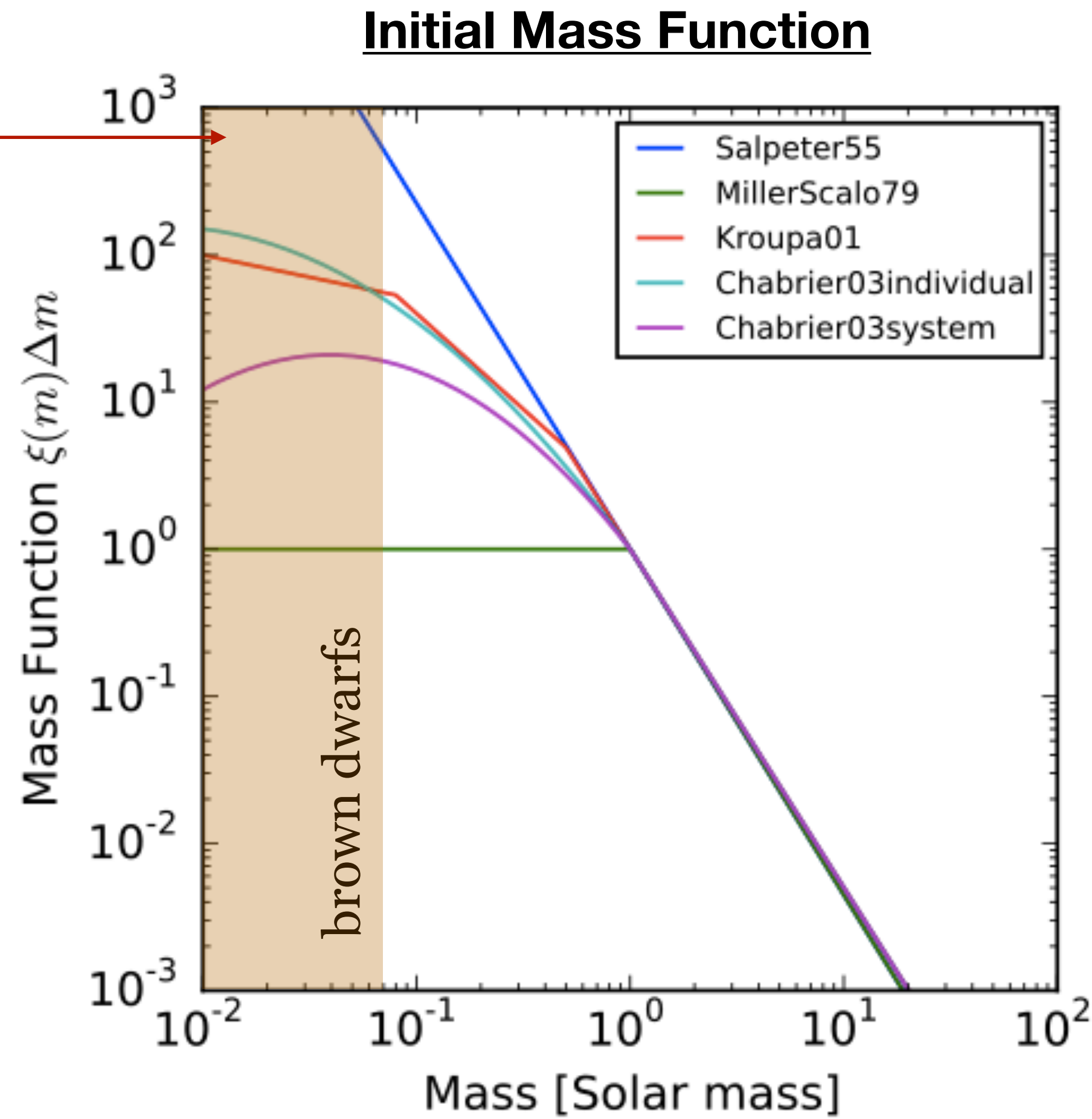
weak gravitational lensing

Weak Lensing extends the RAR to very low accelerations



Microlensing searches for dark matter

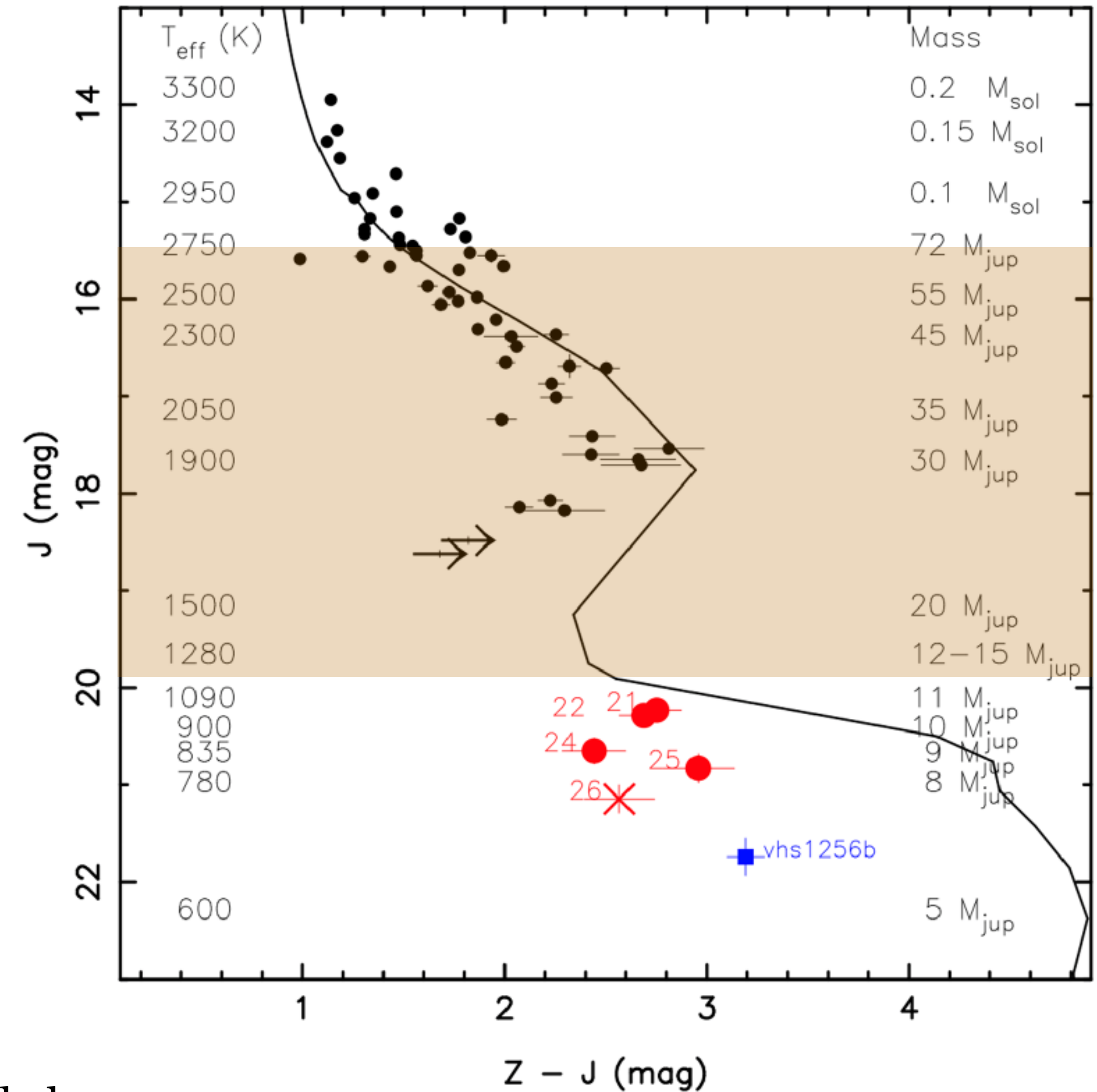
there could be a lot of mass in brown dwarfs, depending on the IMF



$$M_{BD} < 0.07 M_{\odot}$$

brown dwarfs are failed stars below the hydrogen burning limit

Geosciences 2018, 8(10), 362; <https://doi.org/10.3390/geosciences8100362>



Microlensing surveys: MACHO, EROS, OGLE

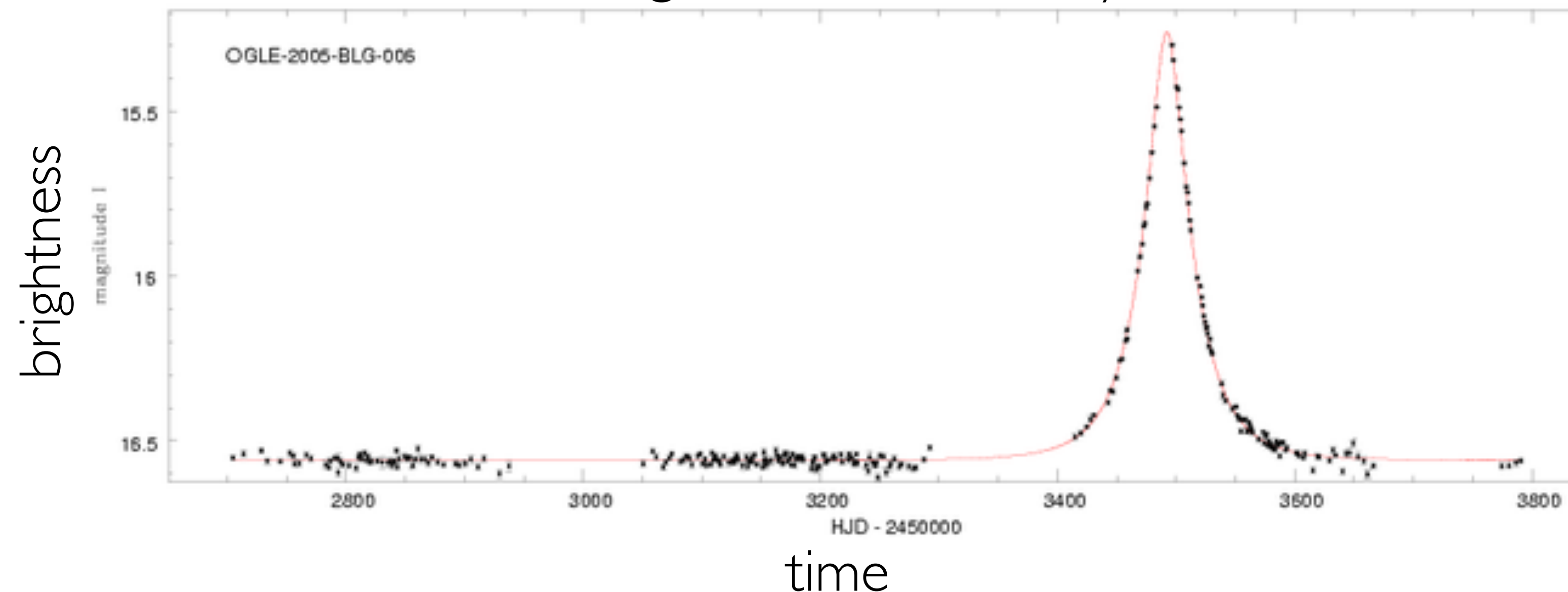
Monitor regions of dense star fields: LMC/SMC/Galactic Center

Watch for microlensing events due to intervening masses

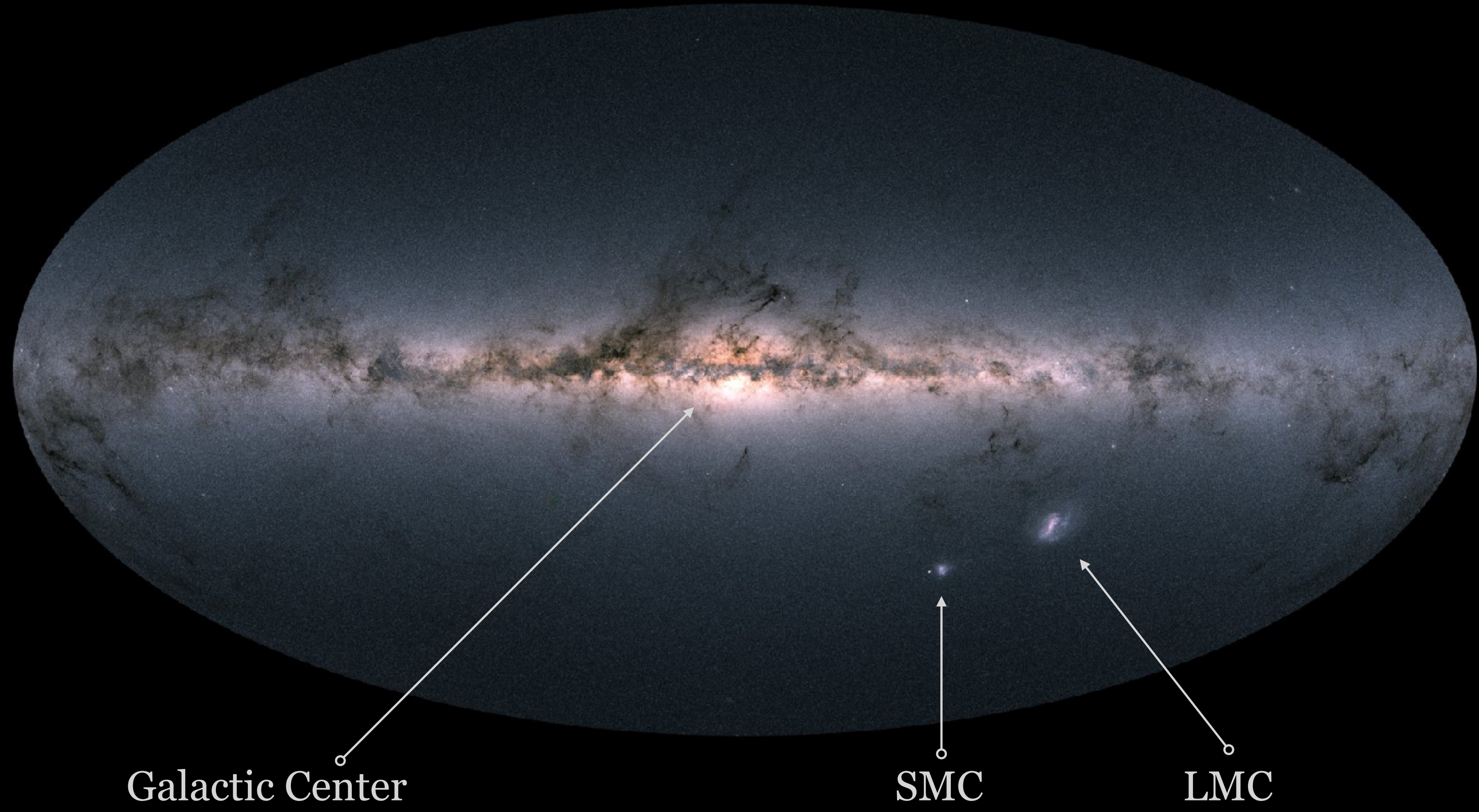
Sensitive to brown dwarfs & stellar mass objects,
including neutron stars and black holes.

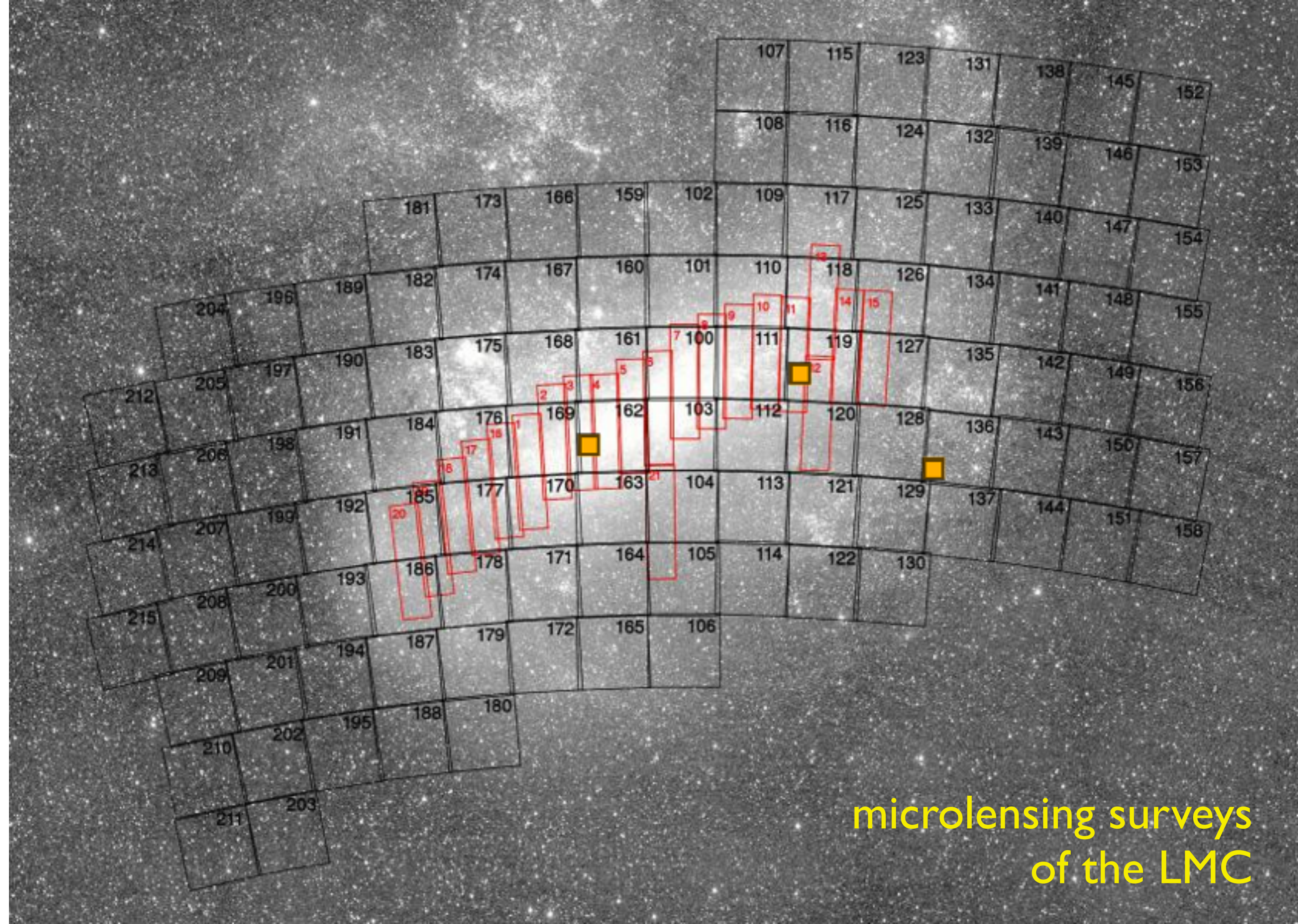
Don't detect the object itself, but the light bending effect it causes on
background stars

microlensing event observed by OGLE



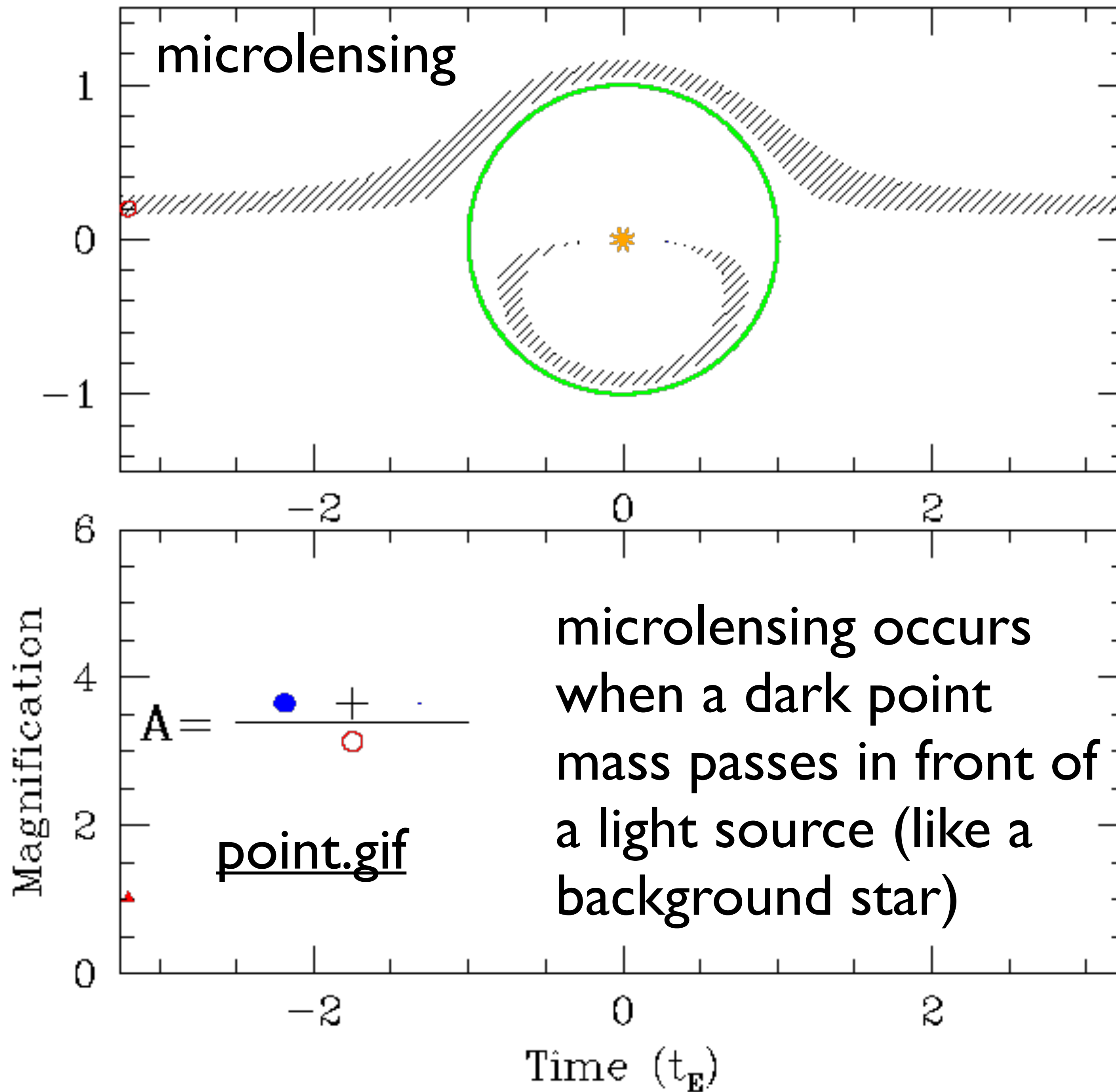
Milky Way in the optical (all sky Gaia data)

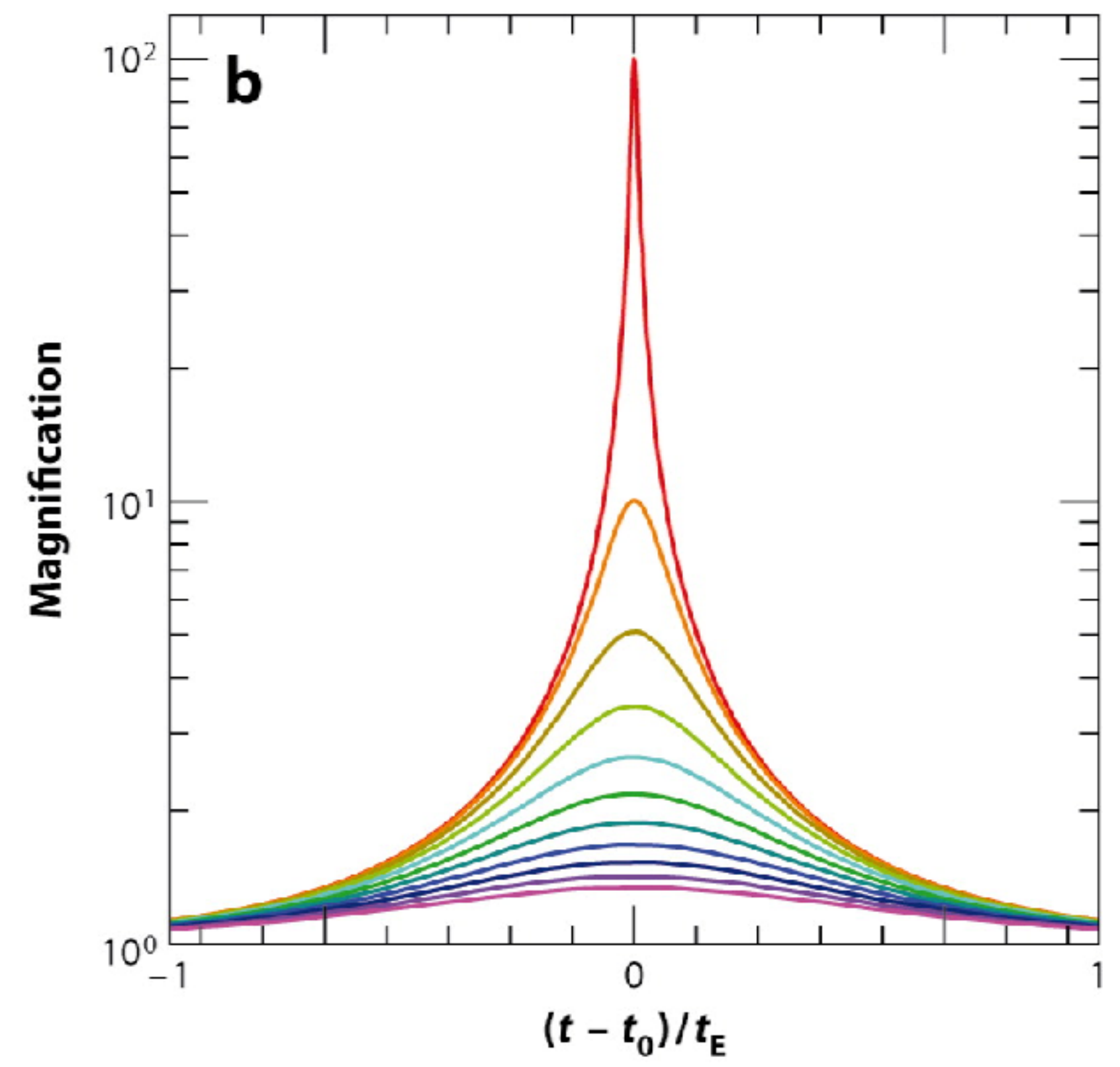
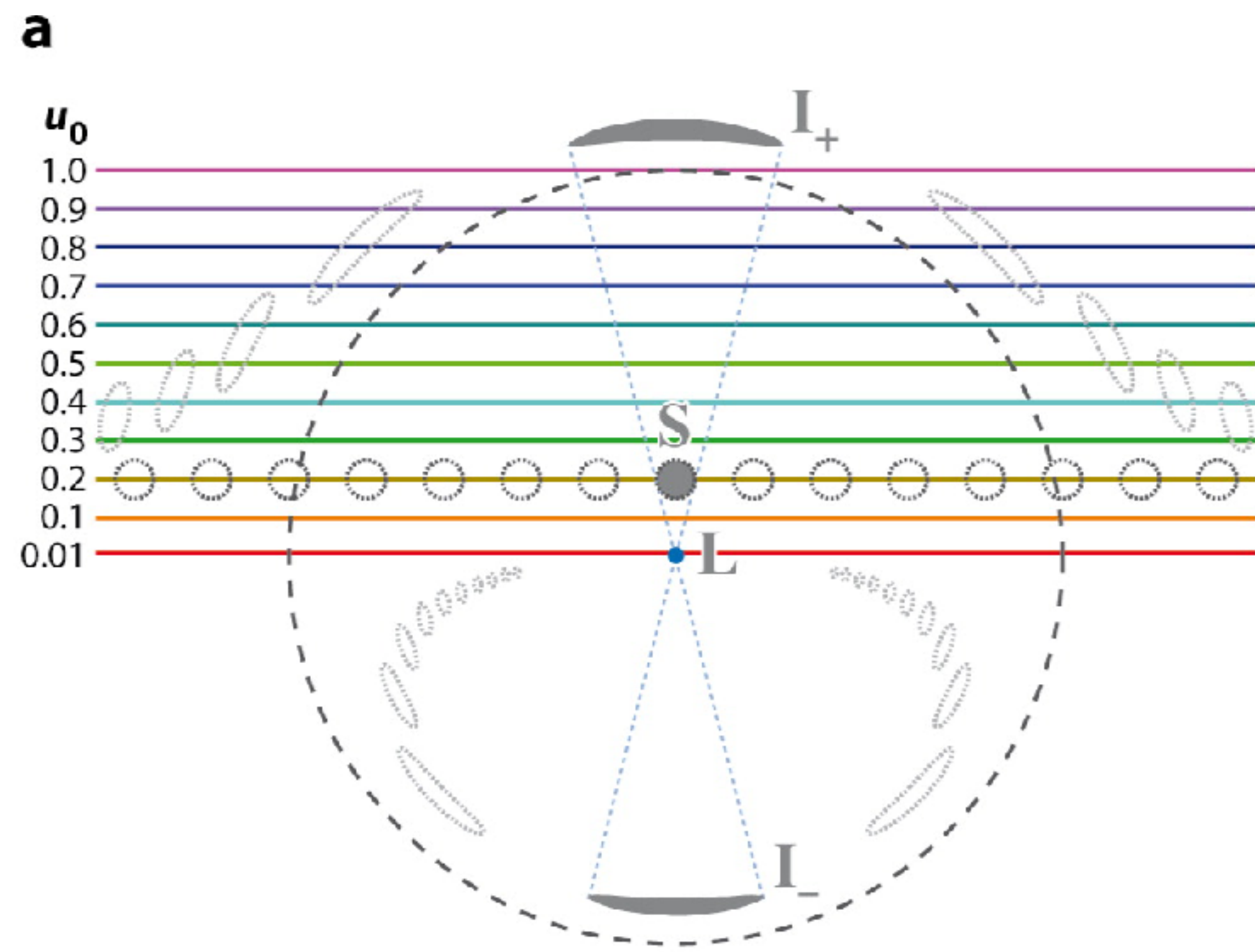




microlensing surveys
of the LMC

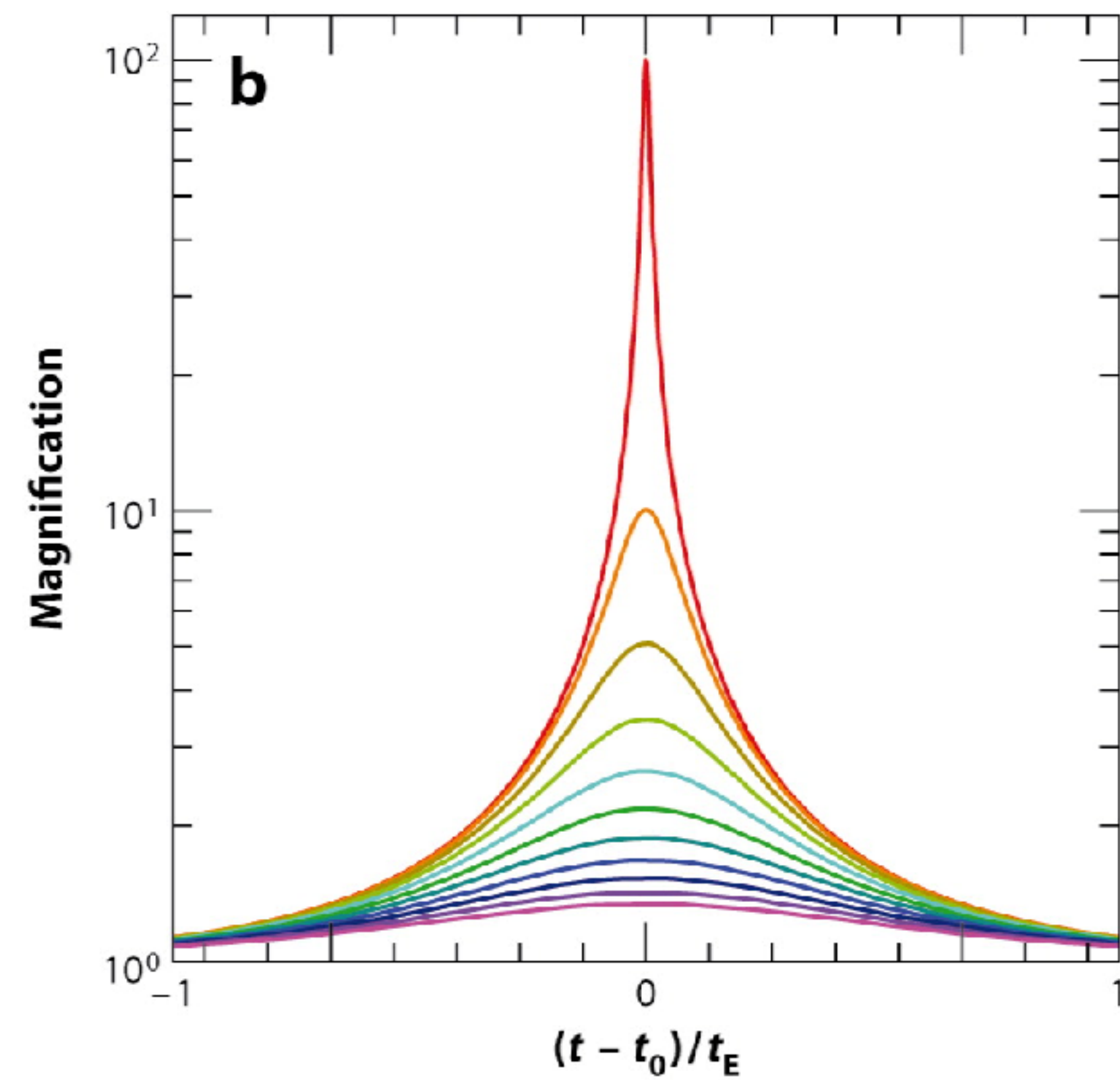
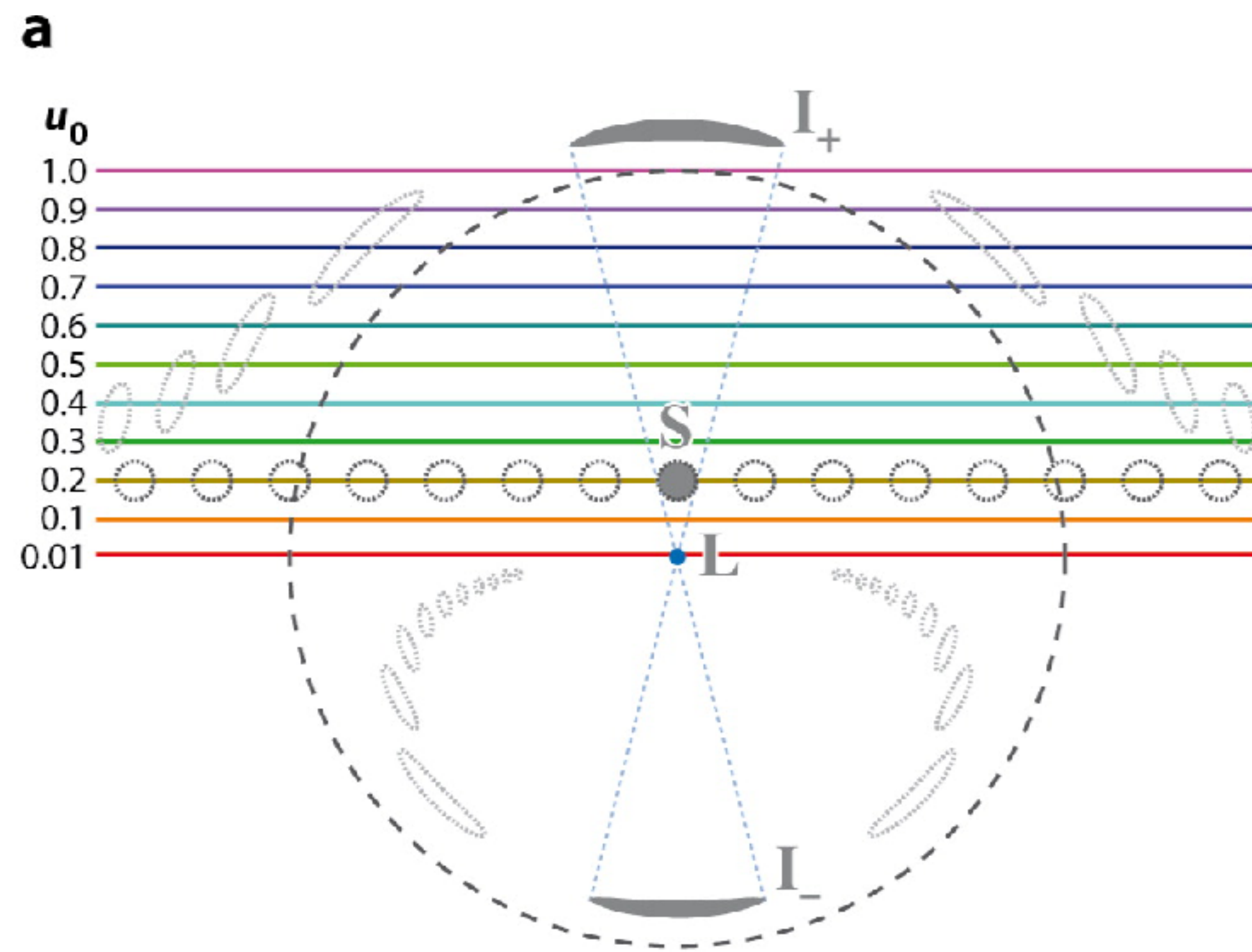
SMALL SCALES





Amplification: $A = \frac{2 + u^2}{u\sqrt{4 + u^2}}$ $u = \frac{\theta}{\theta_E}$

Einstein ring radius: $\theta_E = \sqrt{\frac{4GM}{c^2} \frac{D_{LS}}{D_L D_S}}$

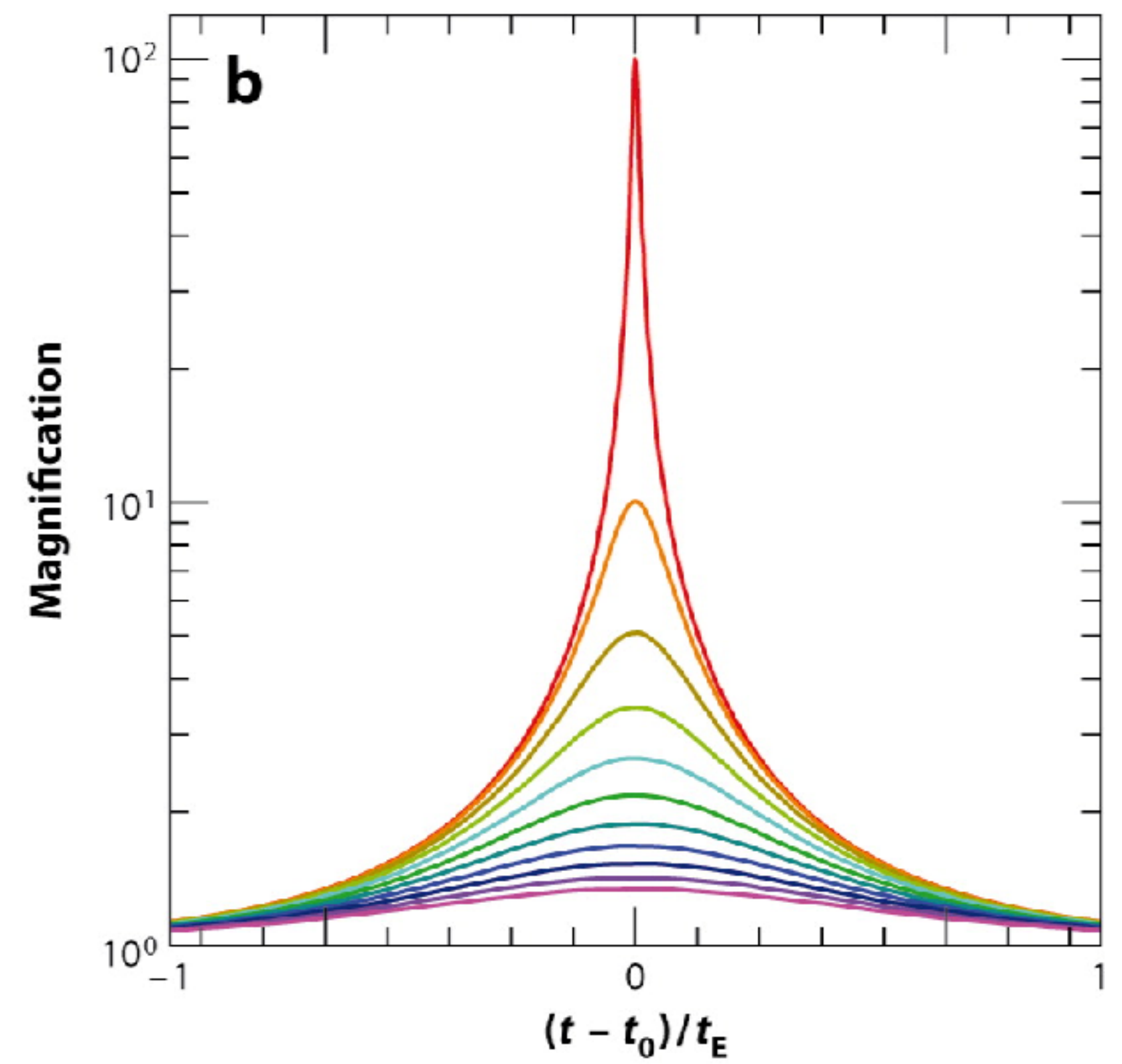
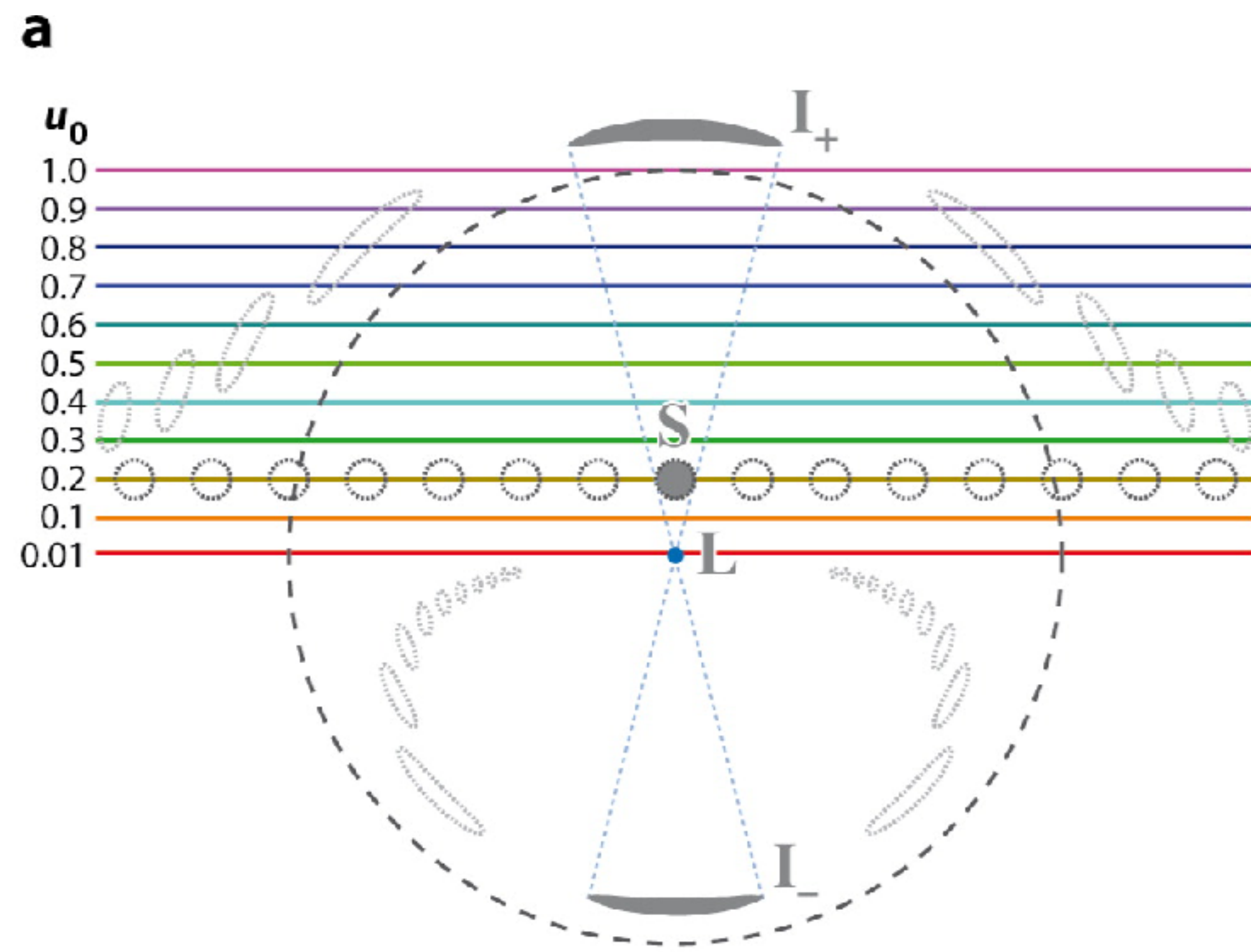


AR Gaudi BS. 2012.
 Annu. Rev. Astron. Astrophys. 50:411–53

$$t_E = \frac{\theta_E}{\mu_{rel}} \quad \text{Einstein crossing time: time to cross Einstein ring.}$$

Einstein ring radius:
$$\theta_E = \sqrt{\frac{4GM}{c^2} \frac{D_{LS}}{D_L D_S}} \approx 10^{-4} \text{ arc seconds for a brown dwarf half way to the LMC}$$

$M = 0.06 M_\odot \quad D_L = D_{LS} = 25 \text{ kpc}$



Lensing optical depth:

$$\tau = \frac{4\pi G}{c^2} D_S^2 \int_0^{D_S} \rho(x) x(1-x) dx \quad \text{where} \quad x = \frac{D_L}{D_S} \quad \text{for density of lenses} \quad \rho(x)$$

for constant density

$$\tau = \frac{2\pi G \rho}{3c^2} D_S^2$$

for Milky Way dark matter halo

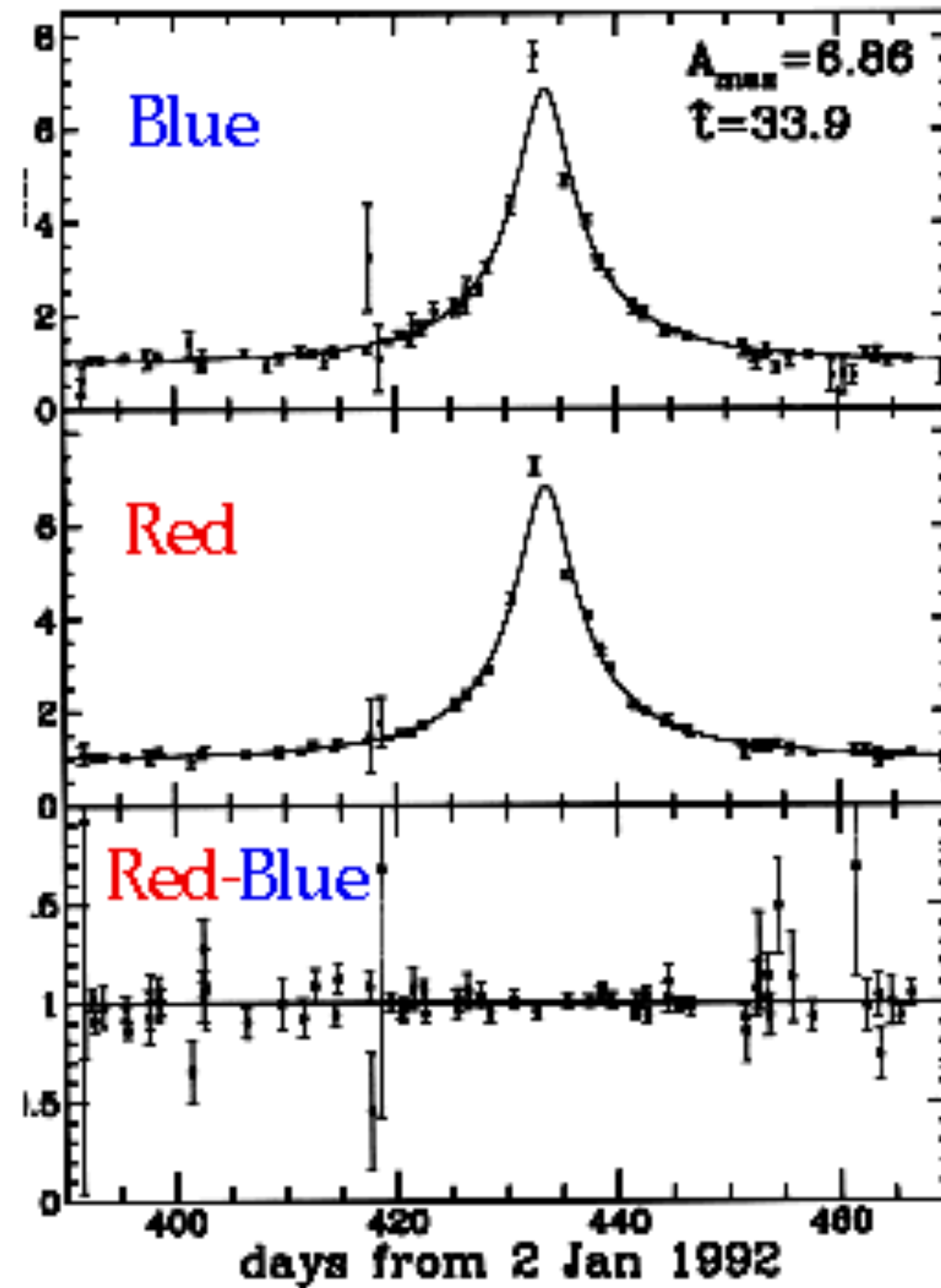
$$\tau = 2\pi \left(\frac{\sigma}{c} \right)^2 \frac{D_L D_{LS}}{R_0 D_S}$$

to the LMC

$$D_L \approx D_{LS} \approx D_S/2$$

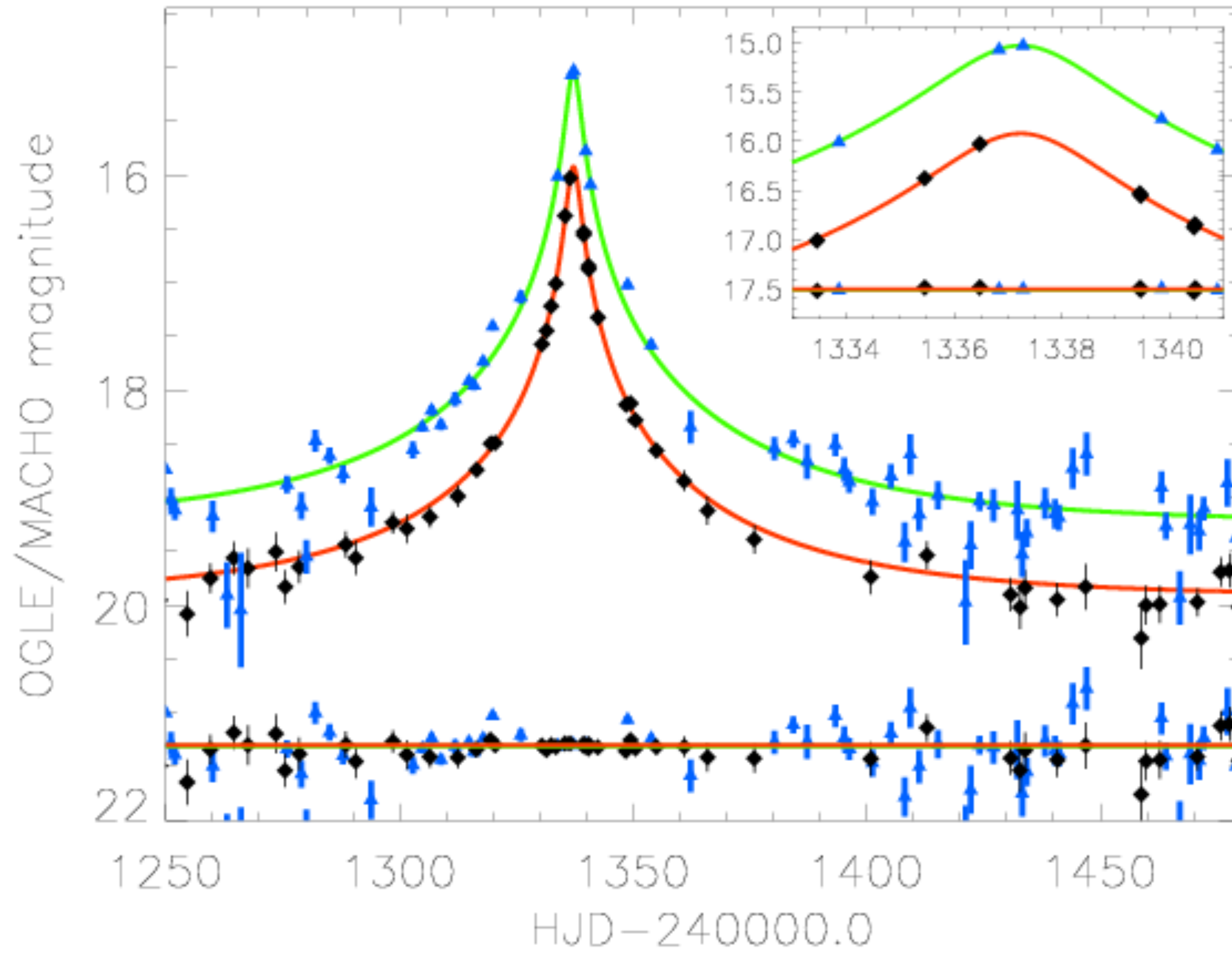
$$D_S = 50 \text{ kpc}$$

microlensing events achromatic



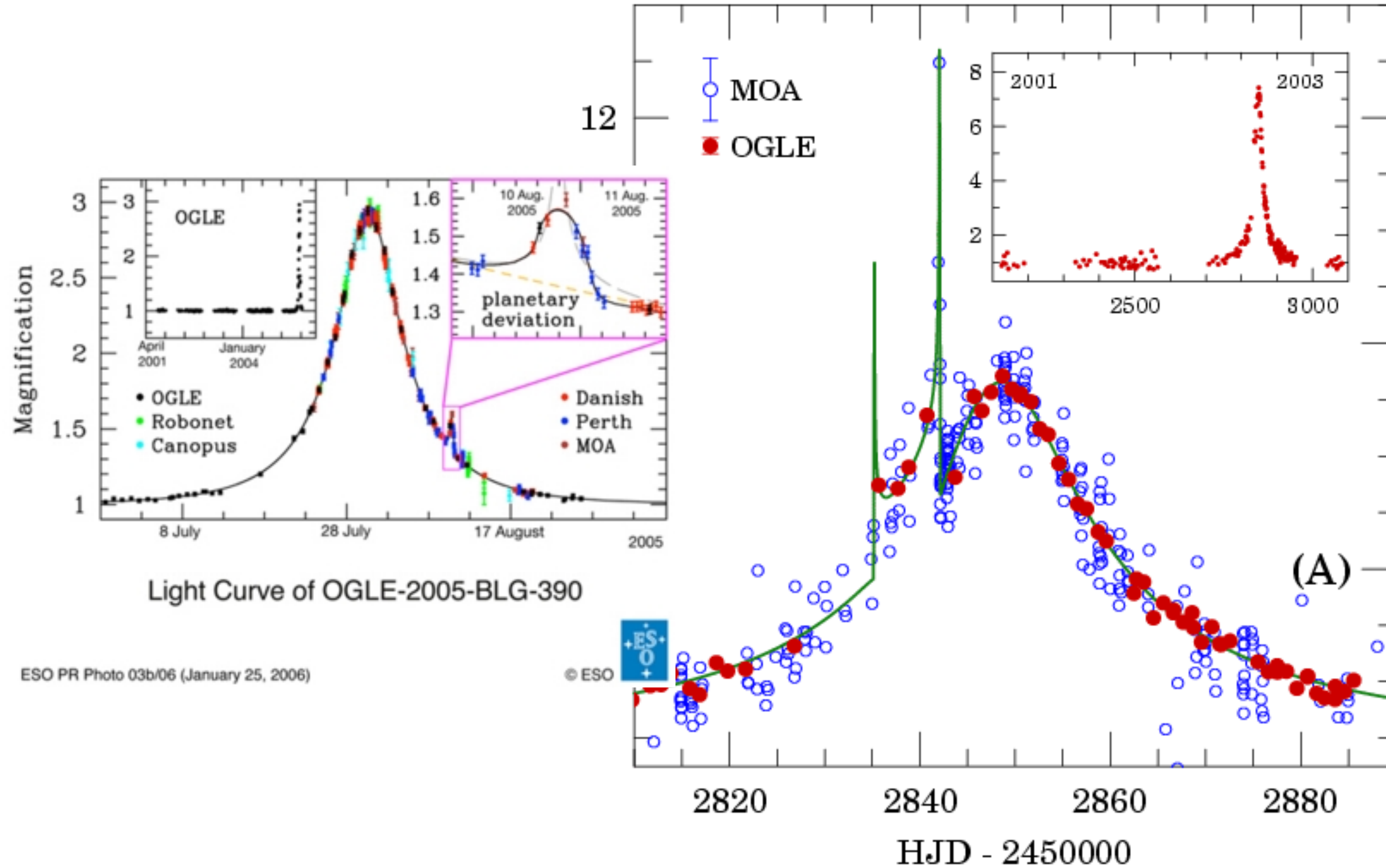
should also be symmetric in time
(unless there is a companion planet)

OGLE-LMC-01



achromatic macho candidate event

Planet detections by microlensing



Number of microlensing events

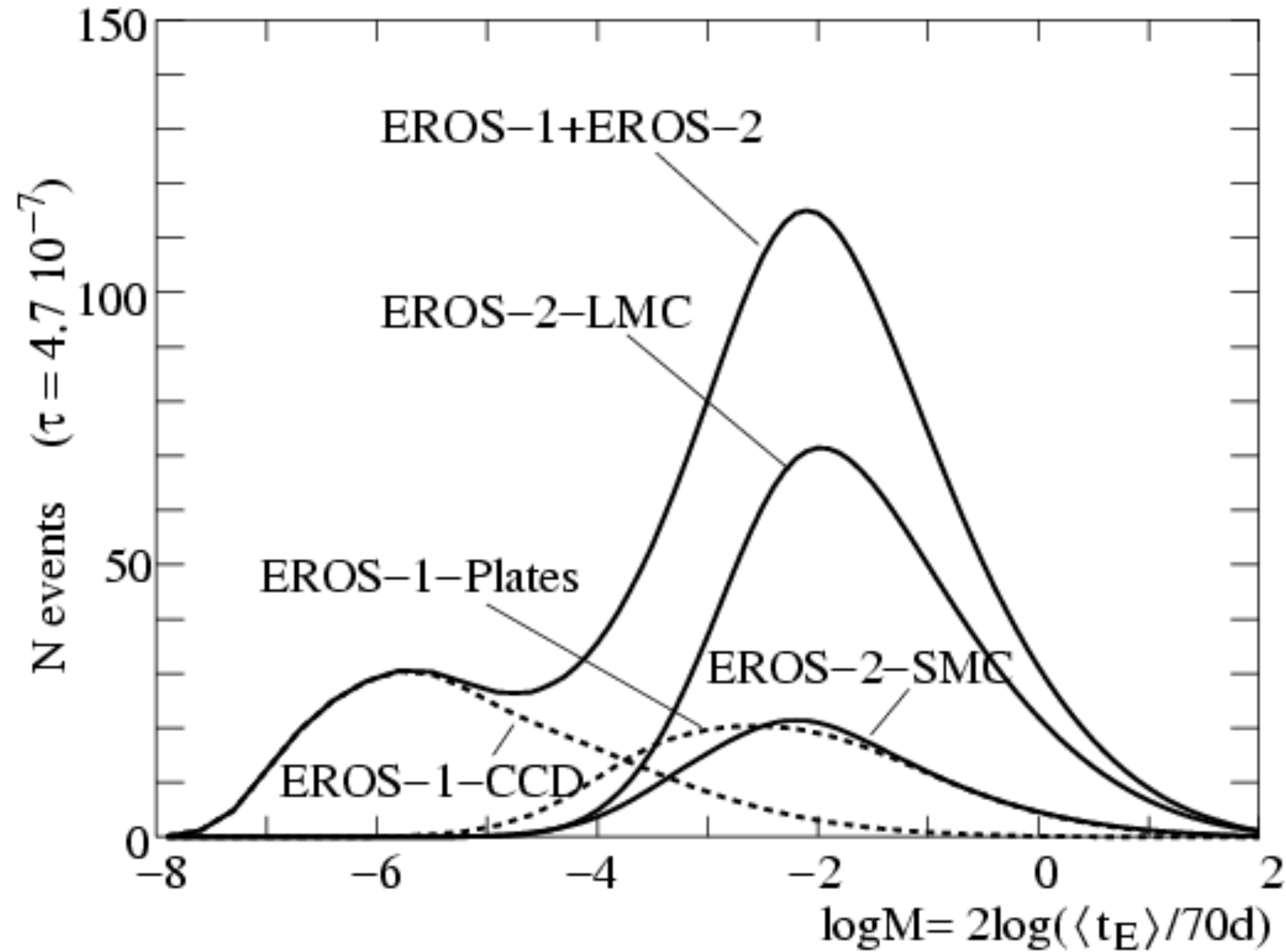
$$N(> A) = \frac{2\tau}{(A^2 - 1) + A\sqrt{A^2 - 1}}$$

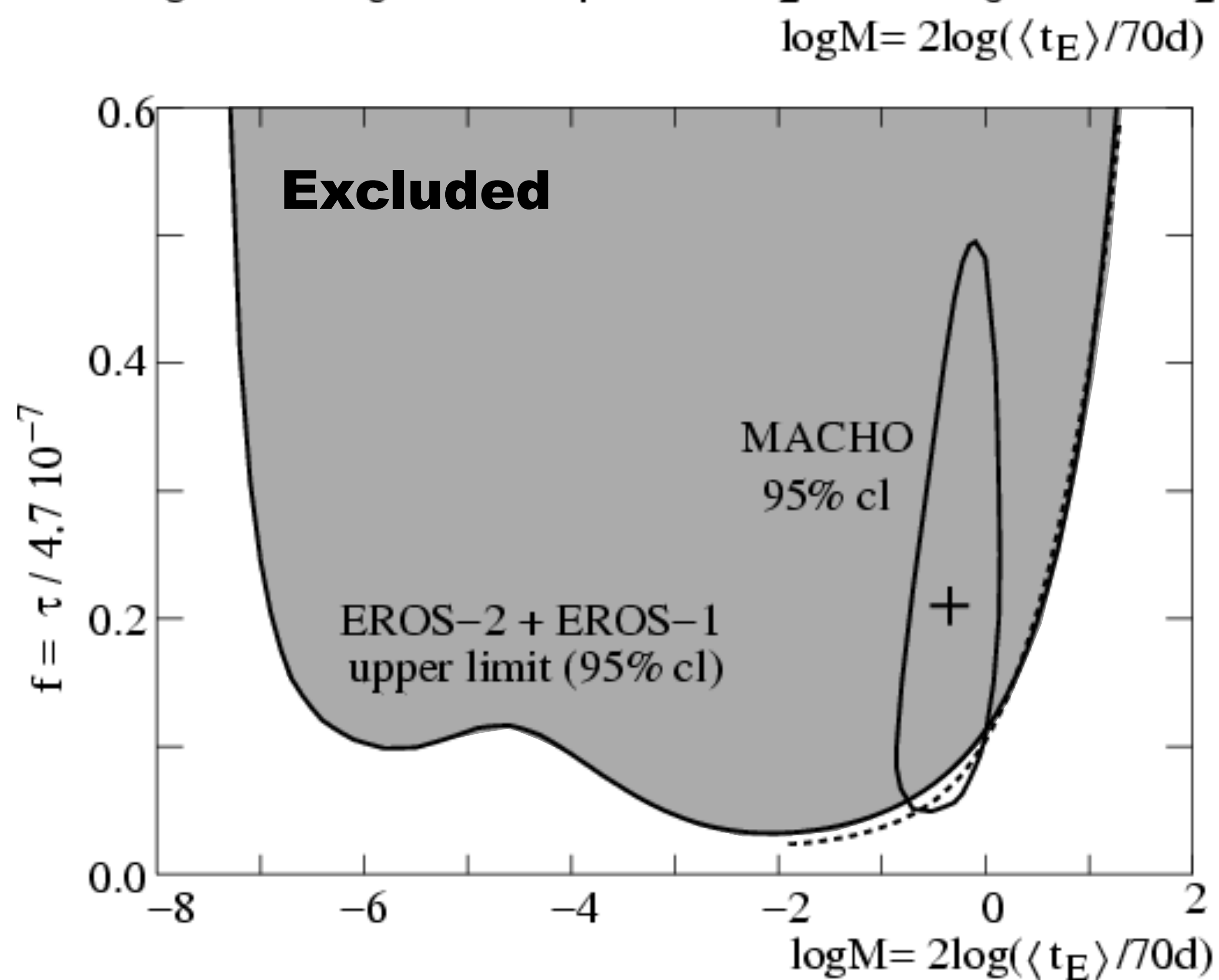
optical depth as a fcn of radius through an isothermal sphere

$$\tau = 2\pi \frac{\sigma_V^2}{c^2} \frac{D_L D_{LS}}{r D_s}$$

optical depth = fraction of the sky covered by Einstein rings

Number of microlensing events expected if all the halo mass is in MACHOs

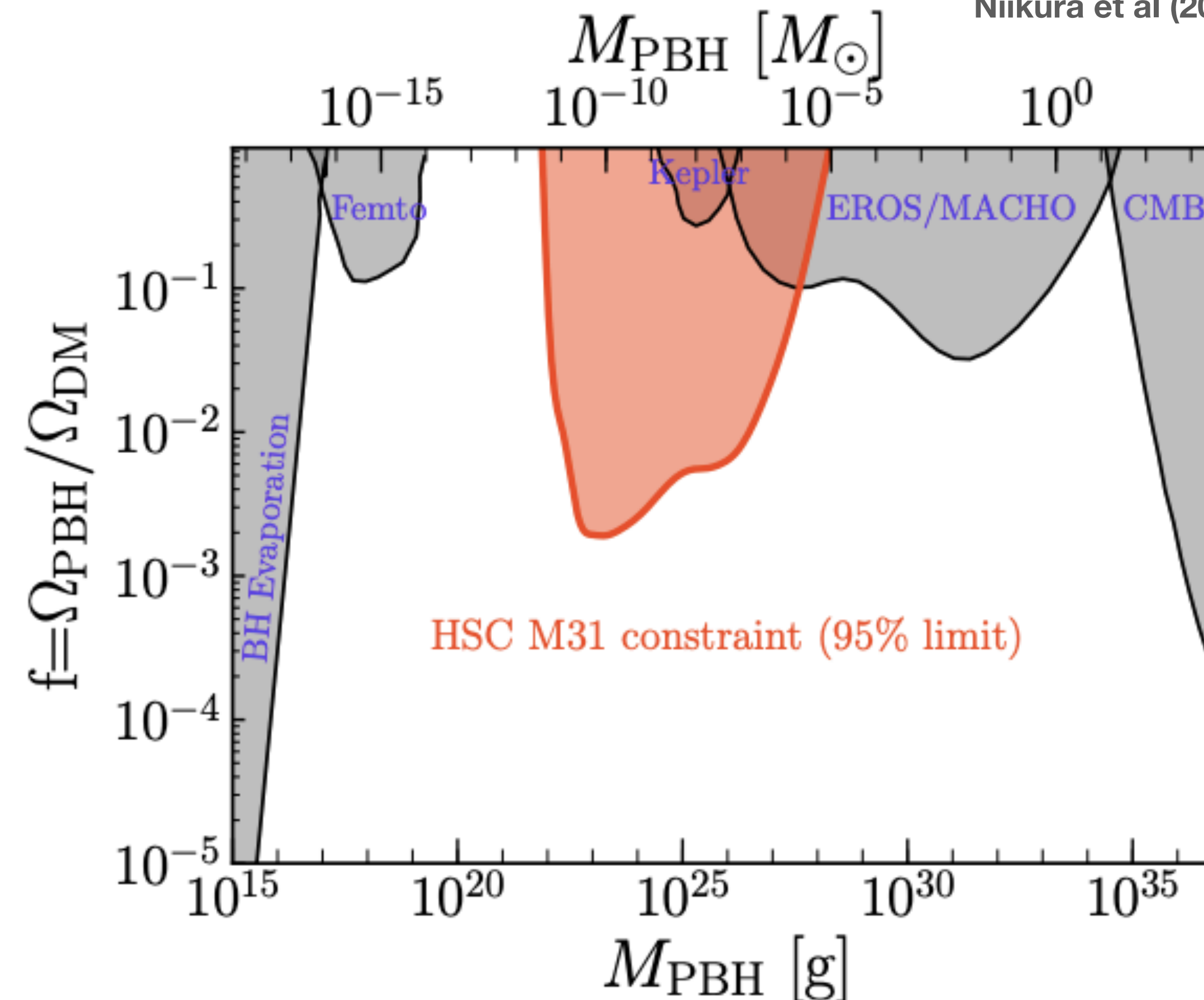




The observed rate of microlensing events leaves no room for the dark matter halo of the Milky Way to be composed of massive compact objects like brown dwarfs or black holes in the mass range $10^{-7} < M < 10$ solar masses.

Subaru study of microlensing towards M31

Niikura et al (2019) Nature Astronomy, 3, 524



The red shaded region corresponds to the 95% C.L. upper bound on the PBH mass fraction to DM in the halo regions of MW and M31, derived from our search for microlensing of M31 stars based on the “single-night” HSC/Subaru data and fills a large gap in the existing constraints by closing the PBH DM window around lunar mass scale. To derive this constraint, we took into account the effect of finite source size, assuming that all source stars in M31 have a solar radius, as well as the effect of wave optics in the HSC r-band filter on the microlensing event (see text for details). The effects weaken the upper bounds at $M < \sim 10^{-7} M_{\odot}$, and give no constraint on PBH at $M < \sim 10^{-11} M_{\odot}$. Our constraint can be compared with other observational constraints as shown by the gray shaded regions: extragalactic γ -rays from PBH evaporation [32], femtolensing of γ -ray burst (“Femto”) [33], microlensing search of stars from the satellite 2-years Kepler data (“Kepler”) [18], MACHO/EROS/OGLE microlensing of stars (“EROS/MACHO”) [15], and the accretion effects on the CMB observables (“CMB”) [34], updated from the earlier estimate [35].

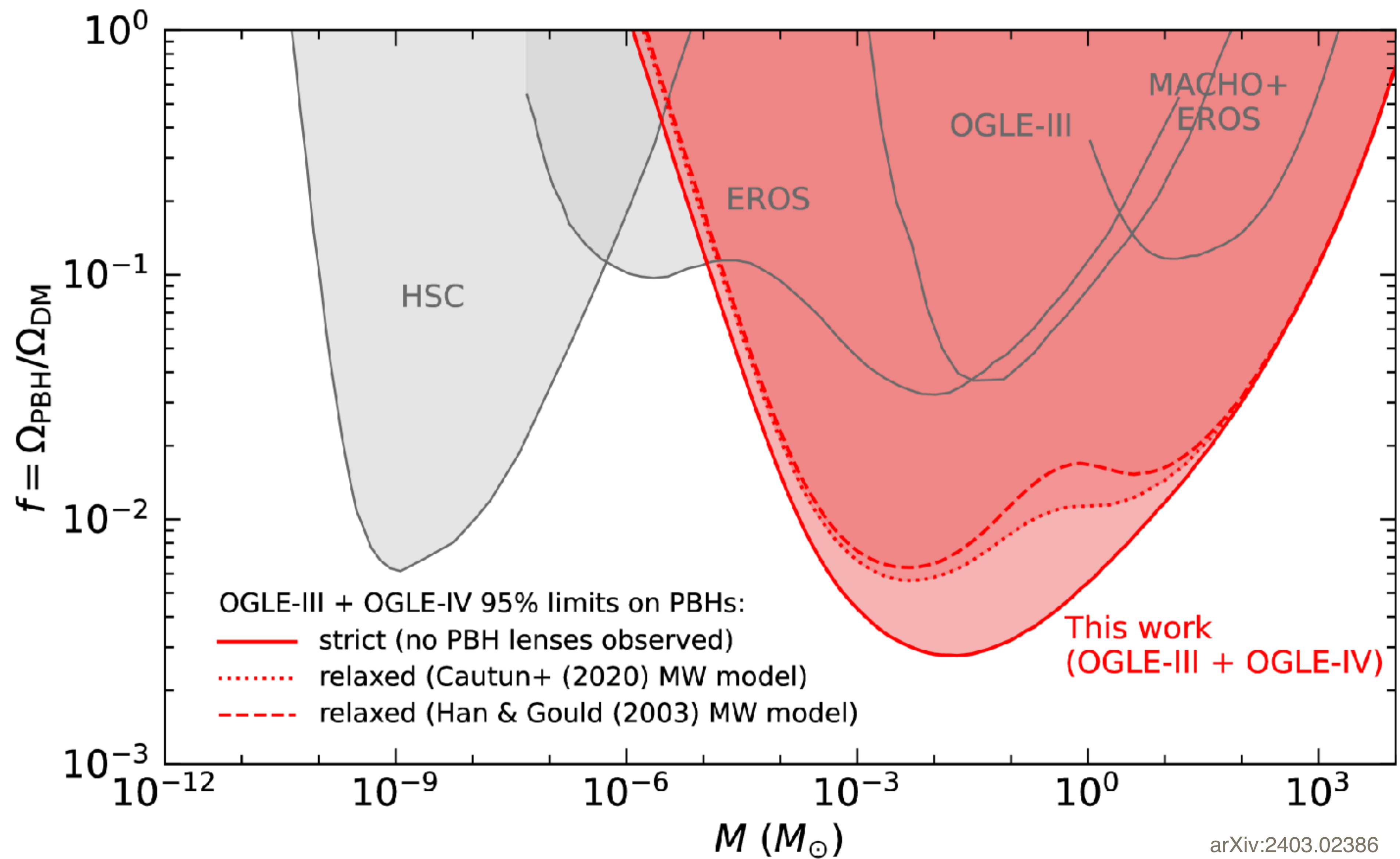
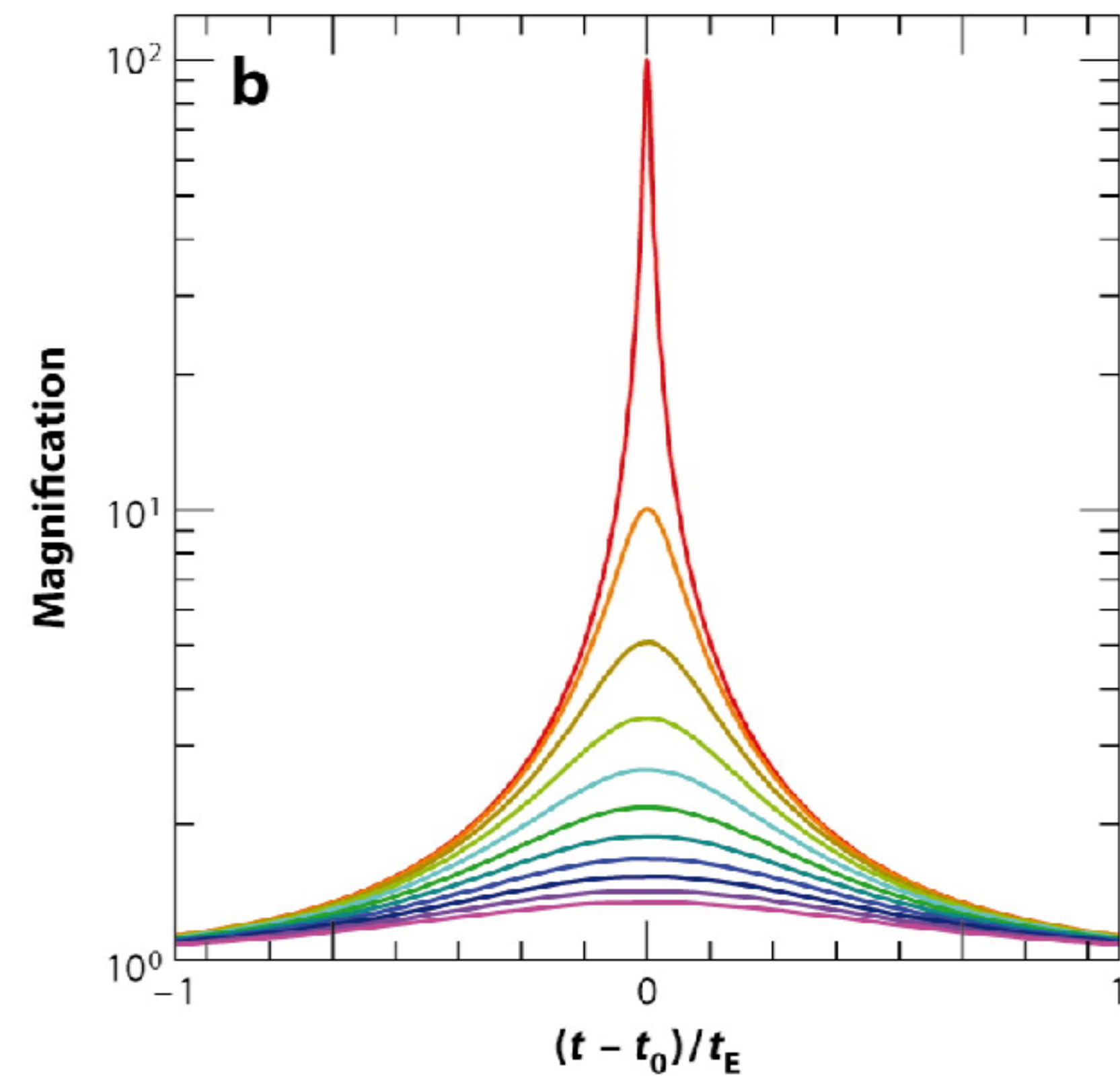
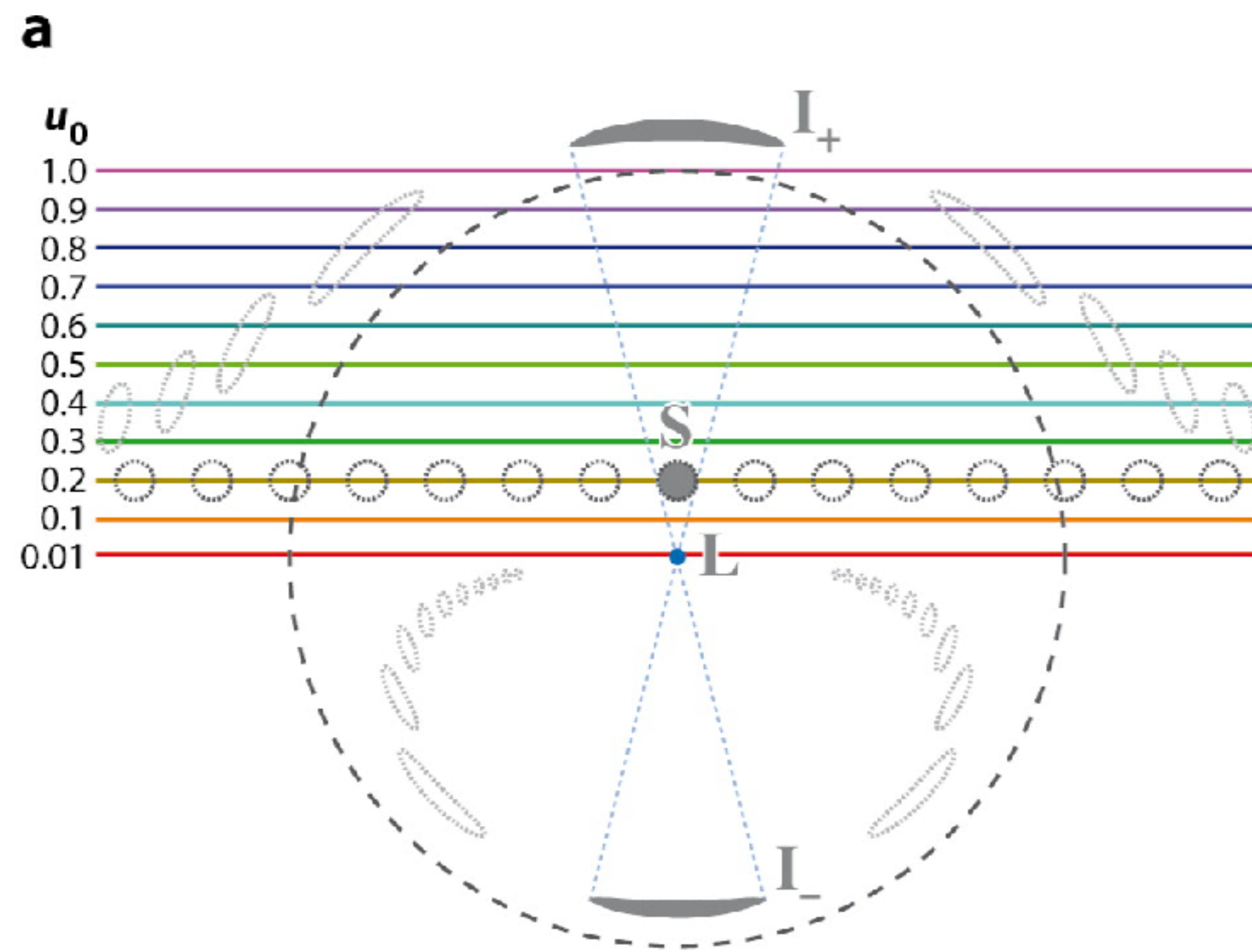


Figure 1: 95% upper limits on PBHs (and other compact objects) as constituents of dark matter. The solid red line marks the limits derived in this paper under the assumption that microlensing events detected by OGLE in the direction of the LMC are due to objects in the LMC itself or the Milky Way disk. If this assumption is relaxed, the limits (dotted and dashed red lines) depend on the choice of the Milky Way disk model ([23] or [24], respectively). The gray lines mark the limits determined by the following surveys: EROS [16], OGLE-III [17] (HSC) [25], and MACHO+EROS [18]. The new limits are publicly available online at https://www.astrouw.edu.pl/ogle/ogle4/LMC_OPTICAL_DEPTH/.

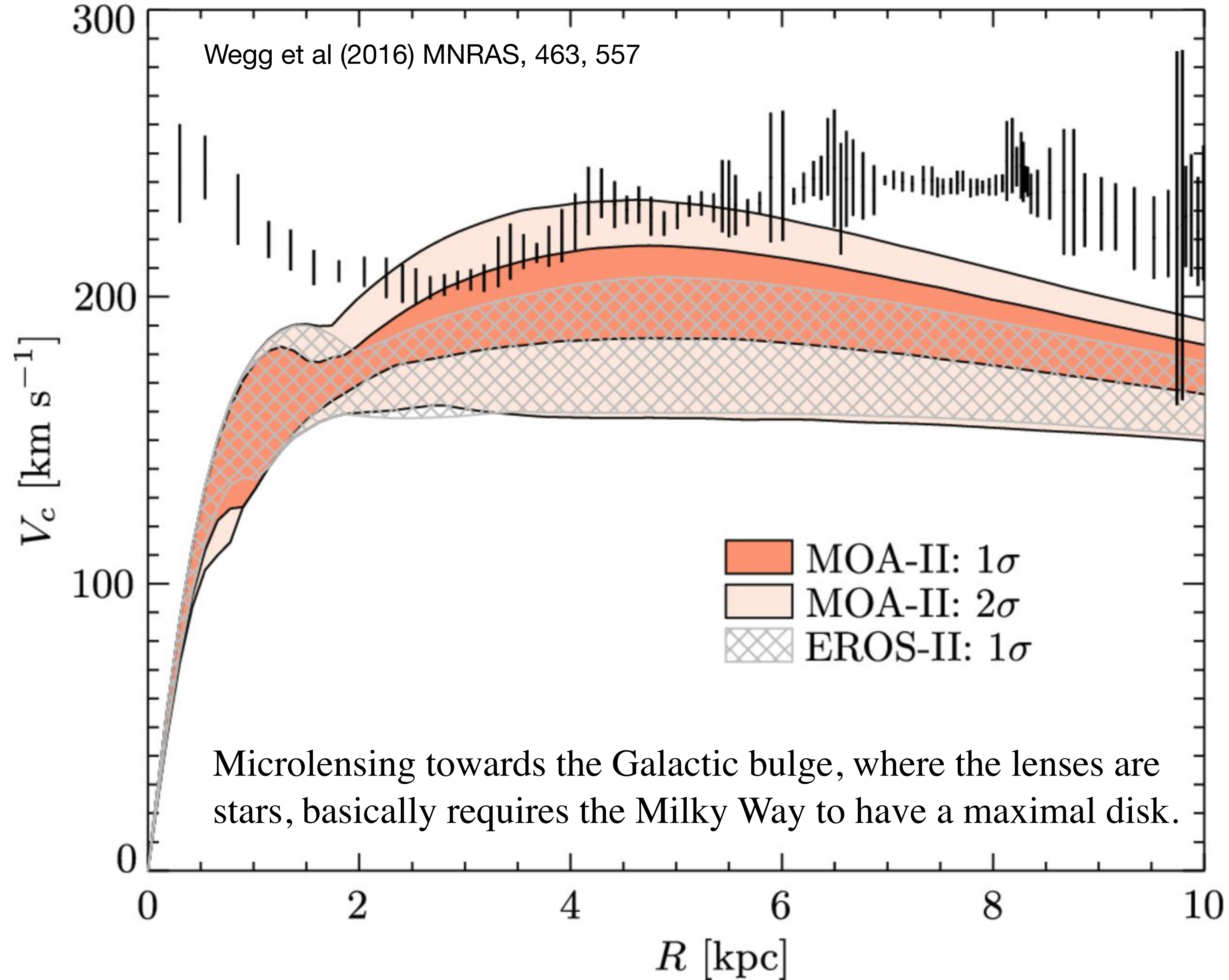


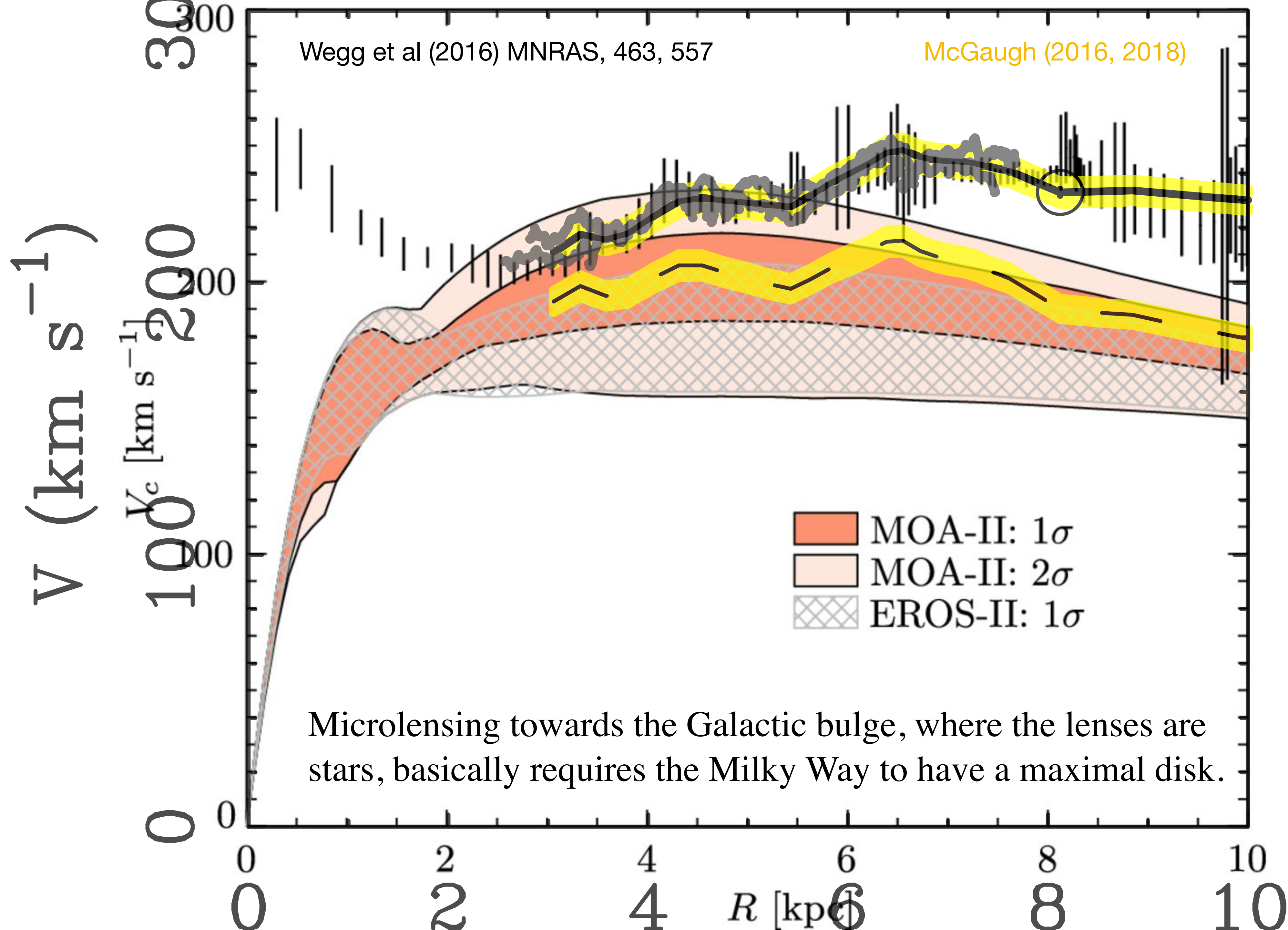
Microlensing towards Galactic Center

$$t_E = \frac{\theta_E}{\mu_{rel}} \quad \text{Einstein crossing time: time to cross Einstein ring.}$$

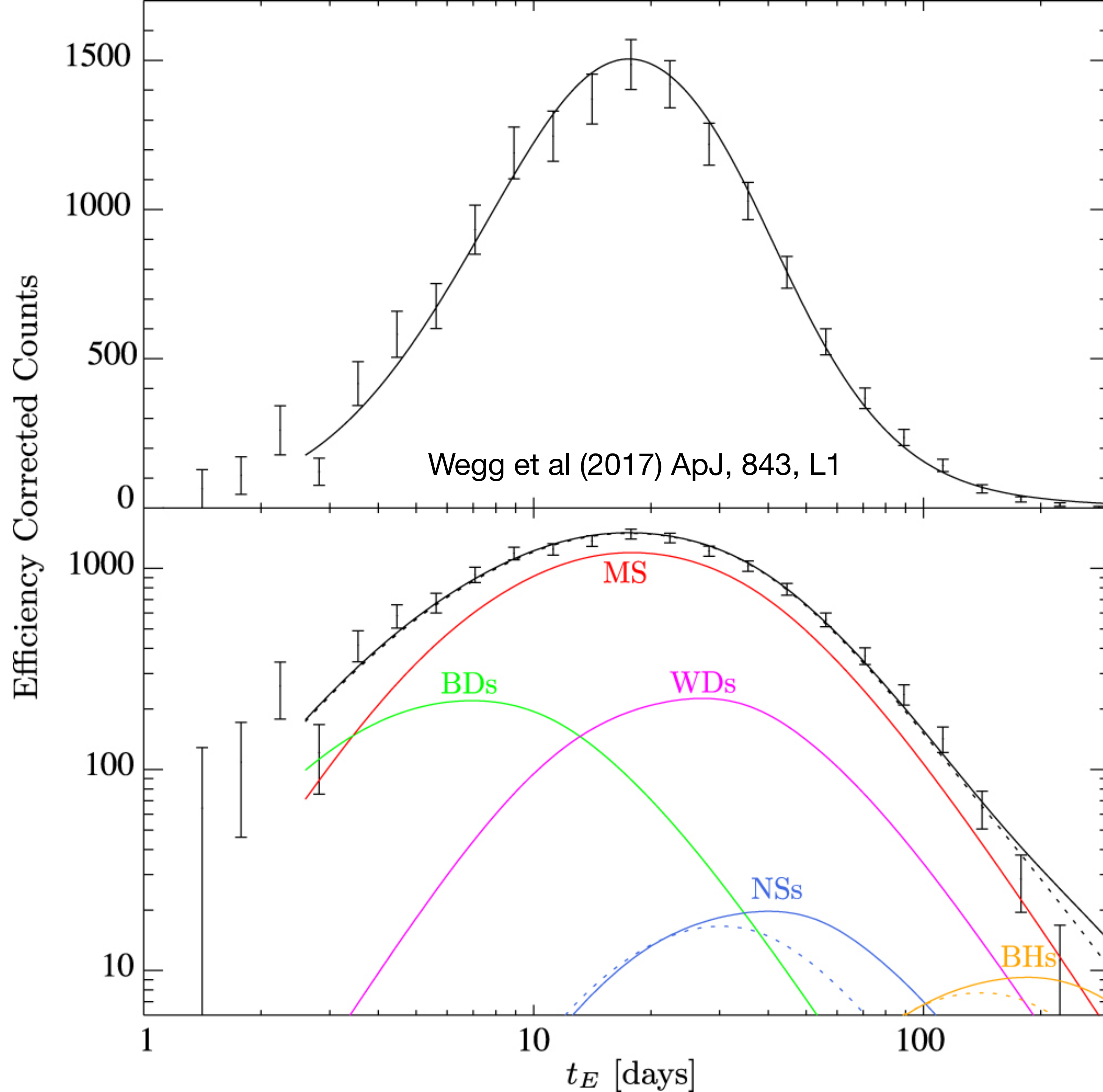
$$t_E \approx (24.8 \text{ days}) \left(\frac{M}{0.5 M_\odot} \right)^{1/2} \left(\frac{\pi_{rel}}{125 \mu\text{as}} \right)^{1/2} \left(\frac{\mu_{rel}}{10.5 \text{ mas yr}^{-1}} \right)^{-1}$$

for lensing events towards the Galactic bulge.

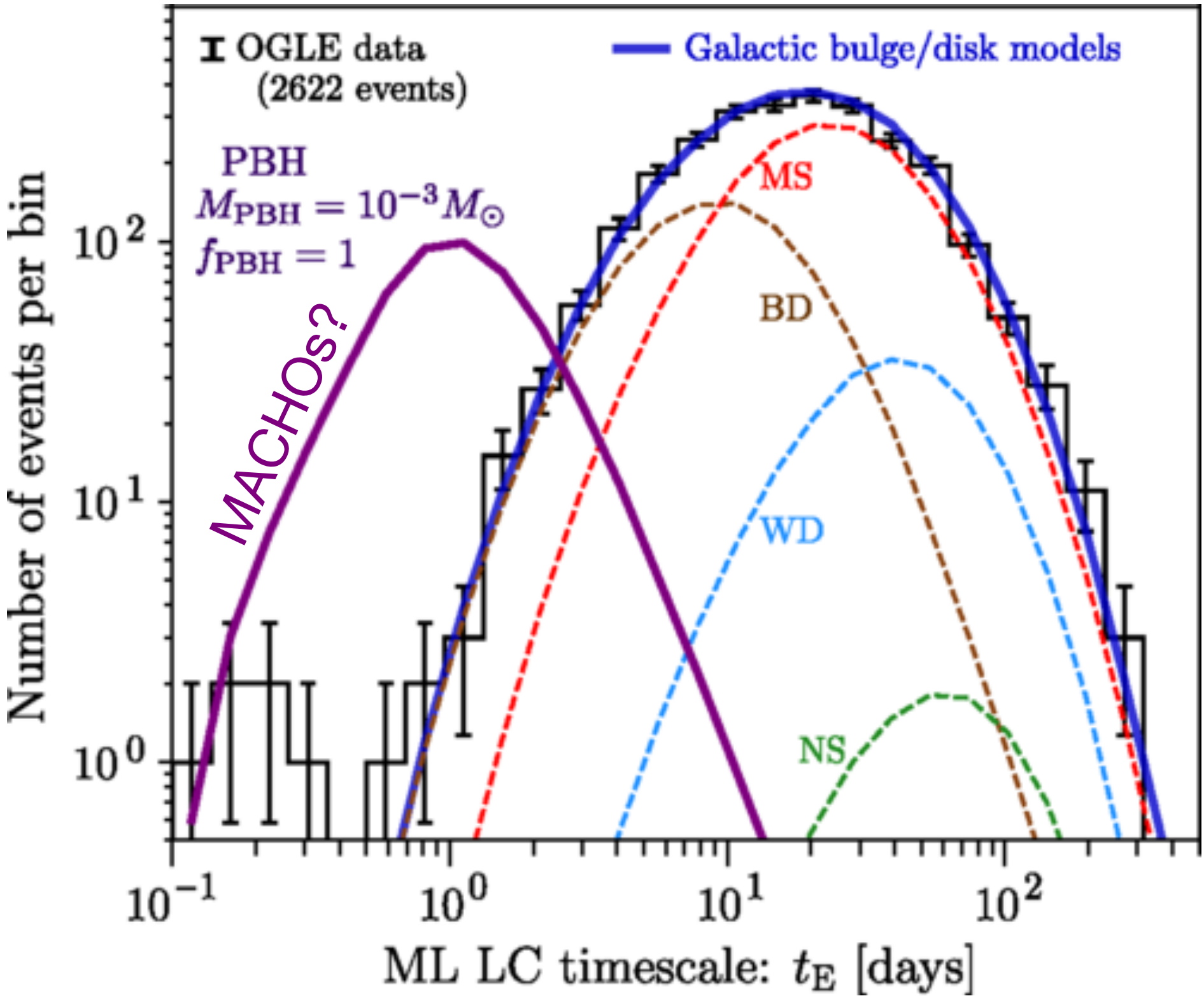




Also constrains the IMF to be basically the same as seen everywhere else.



Microlensing events towards the Galactic Center



well explained by known stars and stellar remnants
without room for extra MACHOs

microlensing summary

- microlensing is rare but routinely detected
- optical depth consistent with known stars & stellar mass objects
- no positive evidence for MACHO type dark matter
- broad range of MACHO masses excluded:

$$10^{-7} < M_{\text{MACHO}} < 10 M_{\odot}$$

basically ruled out